Bosonic Quantum Information

Moritz Fontboté Schmidt

Spring Semester 2026

Acknowledgmenents: Daniel Kienzler/Jonathan Home's lecture on trapped ions. Eugene Tsao, Nils Droftleff for proof-reading the trapped ion part. Alexander Grimm and Jacob Holder for useful input and discussions.

1 Introduction

These are lecture notes for the Bosonic Quantum Information Class that I gave at ETH Zürich together with Alexander Grimm. I gave around 30% of the lectures, such that these lecture notes are not self-contained (hence the chapter numbers that are not following each other), but I added an introduction chapter to smooth the edges. A reader fluent in quantum optics should be able to pick up the subject from here.

1.1 Basics - The Qubit

We remind you of the Pauli operators

$$\hat{X} = \begin{pmatrix} 0 & 1 \\ 1 & 0 \end{pmatrix}, \quad \hat{Y} = \begin{pmatrix} 0 & -i \\ i & 0 \end{pmatrix}, \quad \hat{Z} = \begin{pmatrix} 1 & 0 \\ 0 & -1 \end{pmatrix}$$

$$\sigma_+ = \begin{pmatrix} 0 & 1 \\ 0 & 0 \end{pmatrix}, \quad \sigma_- = \begin{pmatrix} 0 & 0 \\ 1 & 0 \end{pmatrix}$$

$$\begin{aligned} \hat{\sigma}_\phi &= \cos(\phi)\hat{X} + \sin(\phi)\hat{Y} \\ &= \frac{1}{2}\left((e^{i\phi} + e^{-i\phi})(\sigma_+ + \sigma_-) - i(e^{i\phi} - e^{-i\phi})(-i)(\sigma_+ - \sigma_-)\right) \\ &= \frac{1}{2}\left((e^{i\phi} + e^{-i\phi})(\sigma_+ + \sigma_-) - (e^{i\phi} - e^{-i\phi})(\sigma_+ - \sigma_-)\right) \\ &= \frac{1}{2}\left(\sigma_+ e^{-i\phi} + \sigma_- e^{i\phi}\right) \end{aligned}$$

1.2 Basics - The Quantum Harmonic Oscillator

We define the Hamiltonian as

$$\hat{H} = \hbar\omega\left(\hat{a}^\dagger\hat{a} + \frac{1}{2}\right) = \frac{\hbar\omega}{2}(\hat{p}^2 + \hat{q}^2)$$

with $[\hat{a}, \hat{a}^\dagger] = 1$ and $[\hat{q}, \hat{p}] = i$. To go to physical properties, we have

$$\hat{Q} = \left(\frac{\hbar}{2m\omega_0}\right)^{1/2}(\hat{a}^\dagger + \hat{a}), \qquad \hat{P} = i\left(\frac{\hbar\omega m}{2}\right)^{1/2}(\hat{a}^\dagger - \hat{a})$$

which are now observables in SI units

We define the the quadratures

$$\hat{q} = \frac{1}{\sqrt{2}}(\hat{a} + \hat{a}^\dagger), \hat{p} = \frac{i}{\sqrt{2}}(\hat{a}^\dagger - \hat{a}), [\hat{q}, \hat{p}] = i$$

which can be inverted to

$$\hat{a} = \frac{1}{\sqrt{2}}(\hat{q} + i\hat{p}), \hat{a}^\dagger = \frac{1}{\sqrt{2}}(\hat{q} - i\hat{p})$$

Note that $\hat{q} = \hat{q}^\dagger$ and $\hat{p} = \hat{p}^\dagger$, they are observables. They are such that $[\hat{q}, \hat{p}] = i$. Note that going from Fock to position can be done by using that

$$\langle q|0\rangle = \pi^{-1/4}\exp(-q^2/2)$$

It is also useful to look at overlaps reflecting the fourier transform ($\hat{p} = -i\partial_q$)

$$\langle p|q\rangle = \frac{1}{\sqrt{2\pi}}e^{-ipq}$$

or expressing one as a function of the other

$$|q\rangle = \frac{1}{\sqrt{2\pi}}\int_{-\infty}^{\infty} e^{-ipq}\,|p\rangle\,dp$$

from which it's then clear that

$$e^{-i\alpha\hat{p}}\,|q\rangle = \frac{1}{\sqrt{2\pi}}\int_{-\infty}^{\infty} e^{-i\alpha p}e^{-ipq}\,|p\rangle\,dp = \frac{1}{\sqrt{2\pi}}\int_{-\infty}^{\infty} e^{-ip(q+\alpha)}\,|p\rangle\,dp = |q+\alpha\rangle$$

1.2.1 Operations: Displacements and Spin Rotations

We remind you of the spin rotations

$$\hat{R}_X(\theta) = \exp\left(-\frac{i\theta}{2}X\right)$$

$$\hat{R}_Y(\theta) = \exp\left(\frac{-i\theta}{2}\hat{Y}\right)$$

And generalized rotation along an axis ϕ_s

$$\hat{R}_{\phi_s}(\theta) = \exp\left(-\frac{i\theta}{2}(\cos(\phi_s)\hat{X} + \sin(\phi_s)\hat{Y})\right)$$

We define the displacement operator as

$$\hat{D}(\alpha) = \exp(\alpha\hat{a}^\dagger - \alpha^*\hat{a})$$

which we can rewrite

$$\alpha\hat{a}^\dagger - \alpha^*\hat{a} = i\sqrt{2}(\mathrm{Im}(\alpha)\hat{q} - \mathrm{Re}(\alpha)\hat{p})$$

and thus

$$\hat{D}(\alpha) = \exp\left(i\sqrt{2}(\mathrm{Im}(\alpha)\hat{q} - \mathrm{Re}(\alpha)\hat{p})\right)$$

We can define translation operator in phase space (note that the argument now is a vector)

$$\hat{D}(\vec{u}) = \exp(i(u_p\hat{q} - u_q\hat{p}))$$

$\vec{u} = (u_q, u_p)^T \in \mathbb{R}^2$

Note:

$$\hat{D}(\vec{u}) = \hat{D}\left(\frac{u_q + iu_p}{\sqrt{2}}\right)$$

2 Phase space

2.1 Motivation

Assume you have a density matrix ρ of an oscillator, and you want to build up an understanding for the state it describes. Of course, one can calculate certain quantities, e.g. the energy ($\mathrm{Tr}(\rho\hbar\omega\hat{a}^\dagger\hat{a})$) and so on, but oscillator states are sufficiently complex that building a way of representing them is helpful and enables building an intuition as well as a different type of understanding than what a pure mathematical treatment alone would reveal. Questions one may ask and answer without calculating are of the type "Why are cat states robust against dephasing noise?", or "How does a certain operation (e.g. Displacement) act on a quantum state", without calculating anything.

For a qubit, the representation used is typically the Bloch sphere, but for oscillators there is a whole family of available functions $f(\alpha) : \mathbb{C} \to \mathbb{C}$ that completely represent the quantum state. (i.e. for which there is a direct mapping $\rho \leftrightarrow f(\alpha)$).

Let's take an example in which we try to identify what states we have by only looking at density matrices. I give you these density matrices in the Fock basis

$$\rho_1 = \begin{pmatrix} 0.648 & 0 & -0.349 & 0 & 0.230 & ... \\ 0 & 0 & 0 & 0 & 0 & ... \\ -0.349 & 0 & 0.188 & 0 & -0.124 & ... \\ 0 & 0 & 0 & 0 & 0 & ... \\ 0.230 & 0 & -0.124 & 0 & 0.082 & ... \\ ... & ... & ... & ... & ... & ... \end{pmatrix}$$

$$\rho_2 = \begin{pmatrix} 0.223 & 0 & 0.369 & 0 & -0.128 & ... \\ 0 & 0 & 0 & 0 & 0 & ... \\ 0.369 & 0 & 0.610 & 0 & -0.211 & ... \\ 0 & 0 & 0 & 0 & 0 & ... \\ -0.128 & 0 & -0.211 & 0 & 0.073 & ... \\ ... & ... & ... & ... & ... & ... \end{pmatrix}$$

What are these states? Sharp eyes might recognize that both only have even components, so maybe they were created Hamiltonians composed only of $\hat{a}^2, (\hat{a}^2)^\dagger$ terms. Indeed, ρ_1 is a squeezed state, generated by the unitary $e^{1/2(\hat{a}^2-(\hat{a}^2)^\dagger)}$. But what about ρ_2? It also has the same structure, however now the second Fock state contains most of the population, so it contains more energy. Both exhibit strong correlations between the Fock states so they are probably not classical states of the oscillator. But what is the difference? You see the problem.

In figure 8 are shown three possible ways of representing state ρ_1. First, the Wigner function that might be familiar from previous lectures, then the Fock state populations (the diagonal elements of the above matrices), and finally the characteristic function, the 2D Fourier transform of the Wigner function that we will cover in detail as it will be important for GKP states.

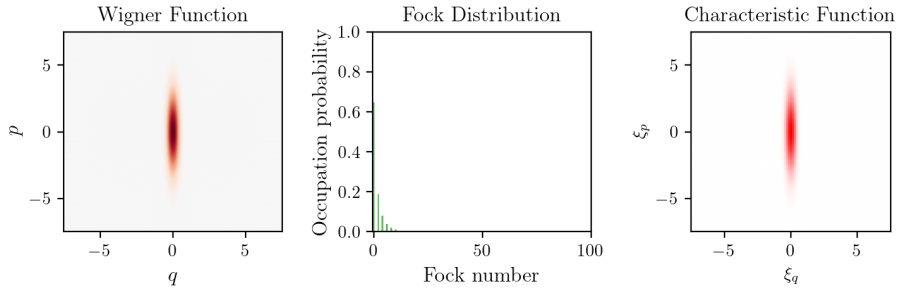

Figure 1: Squeezed state

On the left, observe the Wigner function. You can think of the Wigner function as being a representation of position on the x axis and momentum on the y axis. In classical mechanics, the harmonic oscillator would be represented by a point

in phase space (or a delta function). In quantum mechanics, the commutation relation $[\hat{q}, \hat{p}] = i$ prevents simultaneous knowledge about $\hat{q}$ and $\hat{p}$, hence blurring out the point. It is a quasi-probability distribution, in the sense that if the Wigner function is high in a certain place, it is more likely to find the oscillator in that state when measured in an appropriate basis.

The squeezed state is squeezed along position, meaning that it is very well localized, but its momentum becomes less well defined, which is reflected by the elongated shape of the Wigner function along p. In the center, the Fock state populations as shown as a histogram, and on the right, the characteristic function of the squeezed state, note it also has a squeezed shape, more on that later.

Now, ρ_2 presents itself as shown on figure 2. Notice that it is a squeezed cat state: we have a superposition of left and right displaced squeezed states. Here the fact that there is no odd Fock state in the population has a different reason. The state has a symmetry around the origin, hence only even Fock states represent the state. (remember that Fock states are Gaussians with Hermite polynomials)

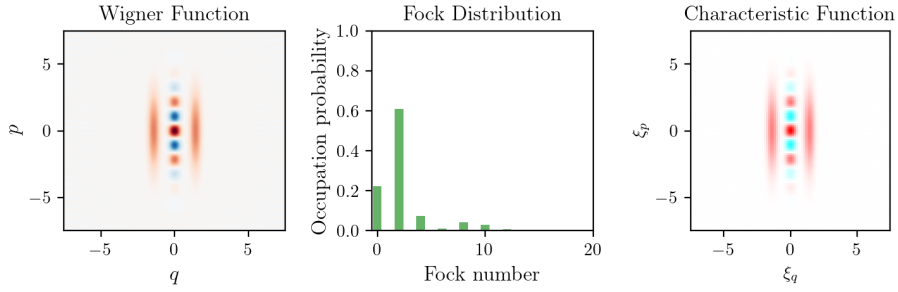

Figure 2: Squeezed cat

The representation reveals more structure than we could read off the density matrix. In the following, we define formally the different phase-space representations.

2.2 Wigner function

Definition We define the Wigner function of the state ρ as

$$W(q,p) = \frac{1}{\pi}\int_{-\infty}^{\infty} \langle q-y|\hat{\rho}|q+y\rangle e^{2ipy} dy$$

or alternatively as

$$W(q,p) = \frac{1}{\pi}\mathrm{Tr}\left[\hat{\rho}\hat{D}(\alpha)\hat{\Pi}\hat{D}^{\dagger}(\alpha)\right]$$

where $\hat{\Pi}$ is the parity operator $e^{i\pi\hat{a}^\dagger\hat{a}}$ and $\alpha = \frac{1}{\sqrt{2}}(q+ip)$.

Properties The Wigner function is always real-valued, i.e.

$$W(q,p) \in \mathbb{R}$$

It is normalized such that

$$\int_{-\infty}^{\infty}\int_{-\infty}^{\infty} W(q,p)dqdp = 1$$

Proof The proof is simple, hence we give it here.

$$\frac{1}{\pi}\iiint \langle q-y|\,\hat{\rho}\,|q+y\rangle\, e^{2ipy}dydqdp$$

using

$$\frac{1}{\pi}\int e^{2ipy}dp = \delta(y)$$

$$\iint W(q,p)dqdp = \iint \langle q-y|\,\hat{\rho}\,|q+y\rangle\,\delta(y)dydq = \int \langle q|\,\hat{\rho}\,|q\rangle\,dq = 1 \quad \square$$

In this proof, it also becomes apparent that one can calculate the marginal $|\psi(q)|^2$ by integrating along p:

$$\int W(q,p)dp = \langle q|\,\hat{\rho}\,|q\rangle = |\psi(q)|^2$$

Similarly, one can show that

$$\int W(q,p)dq = |\tilde{\psi}(p)|^2.$$

The Wigner function is upper and lower bounded

$$|W(q,p)| < \frac{1}{\pi}.$$

It is possible to calculate the overlap of two density matrices by calculating the Wigner function overlap

$$\mathrm{Tr}[\hat{\rho}_1\hat{\rho}_2] = 2\pi\iint W_1(q,p)W_2(q,p)dqdp$$

with W_i the Wigner function of $\hat{\rho}_i$. A consequence is that one can calculate the purity of a state by using the Wigner function

$$\mathrm{Tr}[\rho^2] = 2\pi\iint W^2(q,p)dqdp$$

2.3 Characteristic Function

The characteristic function is the Fourier transform of the Wigner function, and is therefore particularly useful for describing periodic structures. As we will see further in the lecture, the GKP state encodes information into a periodic superposition of states, and hence a peak in characteristic function space will be associated to a certain state, allowing for a very compact description of the contained information in characteristic function space.

Definition The symmetrically ordered characteristic function of a state $\hat{\rho}$ is

$$\chi\left(\xi_q, \xi_p\right) = \chi\left(\beta\right) = \mathrm{Tr}\left[\hat{\rho}\hat{D}(\beta)\right]$$

where $\beta = \frac{1}{\sqrt{2}}(\xi_q + i\xi_p)$ and the displacement operator defined as

$$\hat{D}(\beta) = \exp(\beta\hat{a}^\dagger - \beta^*\hat{a}).$$

β and (ξ_q, ξ_p) are different units and conventions that one will find in the literature and that can be more or less useful depending on the context. We can relate the Wigner and the characteristic function using Fourier transforms by

$$W(q,p) = \frac{1}{(2\pi)^2}\int\int \chi(\xi_q,\xi_p)e^{-i(\xi_p q - \xi_q p)}d\xi_q d\xi_p$$

$$\chi(\xi_q,\xi_p) = \int\int W(q,p)e^{i(\xi_p q - \xi_q p)}dqdp$$

which can also be expressed in displacement units

$$W(\beta) = \frac{1}{\pi^2}\int \chi(\gamma)e^{\beta\gamma^* - \beta^*\gamma}d^2\gamma$$

$$\chi(\beta) = \int W(\gamma)e^{\beta\gamma^* - \beta^*\gamma}d^2\gamma$$

and are functions from $\mathbb{C} \to \mathbb{C}$ to which we can apply tools of complex analysis.

Properties The characteristic function has many properties, here I give a few that we found useful. At the origin, we have

$$\chi(0) = 1$$

this follows from the definition. The characteristic function is well behaved in that it is well bounded,

$$-1 < \chi(\alpha) \leq 1.$$

The function is hermitian symmetric such that

$$\chi(\beta) = \chi^*(-\beta)$$

This is important later on when measuring it, as one does not need to measure the whole space but only half of it. χ can be decomposed into its real part $\mathrm{Re}[\chi]$ and its imaginary part $\mathrm{Im}[\chi]$. The real part encodes the symmetric part of the Wigner function (centered part) while the imaginary part encodes the antisymmetric (displaced) components. This follows from the Hermiticity. Most states we will consider in this lecture are centrally symmetric, such that often times we will only look at the real part of the characteristic function.

A slice through the origin of the characteristic function is Fourier related to the Wigner function marginal/probability density along that axis, i.e.

$$|\psi(q)|^2 = \frac{1}{2\pi}\int_{-\infty}^{\infty} \chi(0,\xi_p)e^{-i\xi_p q}d\xi_p$$

$$|\tilde{\psi}(p)|^2 = \frac{1}{2\pi}\int_{-\infty}^{\infty} \chi(\xi_q,0)e^{i\xi_q p}d\xi_q$$

a useful property when experimentally assessing states by measuring the characteristic function. It is possible to calculate expectation values of operators by measuring the displacement operator's gradient in the center using that

$$-i\frac{\partial\chi}{\partial\xi_q}\bigg|_{\xi=0} = \langle\hat{q}\rangle, \qquad -i\frac{\partial\chi}{\partial\xi_p}\bigg|_{\xi=0} = \langle\hat{p}\rangle.$$

Geometric phase While there is a clear physical meaning and classical analogy in the Wigner function, where a location in phase space corresponds to a state with a given position and momentum, that is not so immediate for the characteristic function. One concept that helps building this understanding is the geometric phase: when two displacements follow paths in phase space that start and end at the same place, their action on a state differs only by a phase factor given by the area between the two paths. In particular, consider the two paths (1) and (2) as shown on figure 3

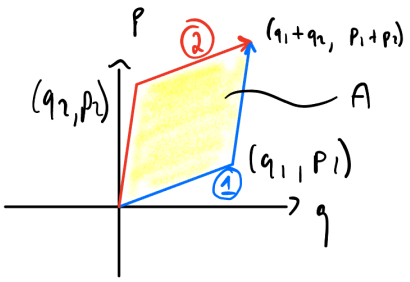

Figure 3: The area enclosed by two paths gives the geometric phase difference between them

A displacement following them can be described by the operators

$$\hat{D}_1 = \hat{D}(q_2, p_2)\hat{D}(q_1, p_1), \quad \hat{D}_2 = \hat{D}(q_1, p_1)\,\hat{D}(q_2, p_2)$$

where I expressed the displacement in quadrature units

$$\hat{D}(q, p) = e^{i(p\hat{q} - q\hat{p})} = \hat{D}\left(\alpha = \tfrac{1}{\sqrt{2}}(q + ip)\right)$$

such that the commutator is given by the area A between the paths,

$$\hat{D}_2 = e^{-i(q_1 p_2 - p_1 q_2)}\hat{D}_1 = e^{-iA}\hat{D}_1$$

where A is the oriented area enclosing the two paths, creating a *geometric* phase between the two paths (it's called geometric because it doesn't depend on the speed of the path, just on the area). The reason we chose the units such that $\alpha = 1/\sqrt{2}(q + ip)$ is such that the area between the two paths is equal to the phase (no factors of 2).

Proof Define $\hat{A} = i(p_1\hat{q} - q_1\hat{p})$ and $\hat{B} = i(p_2\hat{q} - q_2\hat{p})$, such that $\hat{D}(q_k, p_k) = e^{\hat{A}}$ or $e^{\hat{B}}$ respectively. Using $[\hat{q}, \hat{p}] = i$:

$$[\hat{A}, \hat{B}] = -[p_1\hat{q} - q_1\hat{p}, p_2\hat{q} - q_2\hat{p}] = -(-p_1 q_2 + q_1 p_2)[\hat{q}, \hat{p}] = -i(q_1 p_2 - p_1 q_2)$$

This is a number, such that the Baker-Campbell-Hausdorff formula is

$$e^{\hat{A}}e^{\hat{B}} = e^{\hat{A}+\hat{B}+\frac{1}{2}[\hat{A},\hat{B}]} = e^{\hat{A}+\hat{B}}\,e^{\frac{1}{2}[\hat{A},\hat{B}]}$$

giving the composition rule:

$$\hat{D}(q_1, p_1)\hat{D}(q_2, p_2) = \hat{D}(q_1 + q_2, p_1 + p_2)\,e^{-\frac{i}{2}(q_1 p_2 - p_1 q_2)}$$

Applying this to both paths:

$$\hat{D}_1 = \hat{D}(q_2, p_2)\hat{D}(q_1, p_1) = \hat{D}(q_1 + q_2, p_1 + p_2)e^{+\frac{i}{2}A}$$

$$\hat{D}_2 = \hat{D}(q_1, p_1)\hat{D}(q_2, p_2) = \hat{D}(q_1 + q_2, p_1 + p_2)e^{-\frac{i}{2}A}$$

hence

$$\hat{D}_2 = e^{-iA}\,\hat{D}_1$$

where $A = q_1 p_2 - p_1 q_2$ is the oriented area of the parallelogram spanned by the two displacement vectors. □

The phase can be understood similarly to an Aharonov-Bohm phase, where the structure of the commutator $[q, p]$ gives rise to the phase difference between the paths.

2.4 Examples of Wigner and characteristic functions

We now turn to examples of χ.

Ground and displaced states The first state to consider is the ground state. We know that its wavefunction is a Gaussian, such that the Wigner function must also have a Gaussian structure, shown on figure 4 top left. Since χ is its Fourier transform, it will also have a Gaussian structure. Another way to understand it is by recognizing that χ calculates the overlap between the state in question and its displaced self,

$$\chi(\xi_q, \xi_p) = \mathrm{Tr}[\hat{\rho}\hat{D}(\xi_q, \xi_p)] = \langle 0| \left(\hat{D}(\xi_q, \xi_p)\,|0\rangle\right)$$

such that the characteristic function is an overlap integral between two integrals. Since the overlap between two Gaussians is again a Gaussian, so is χ, see figure 4 top right.

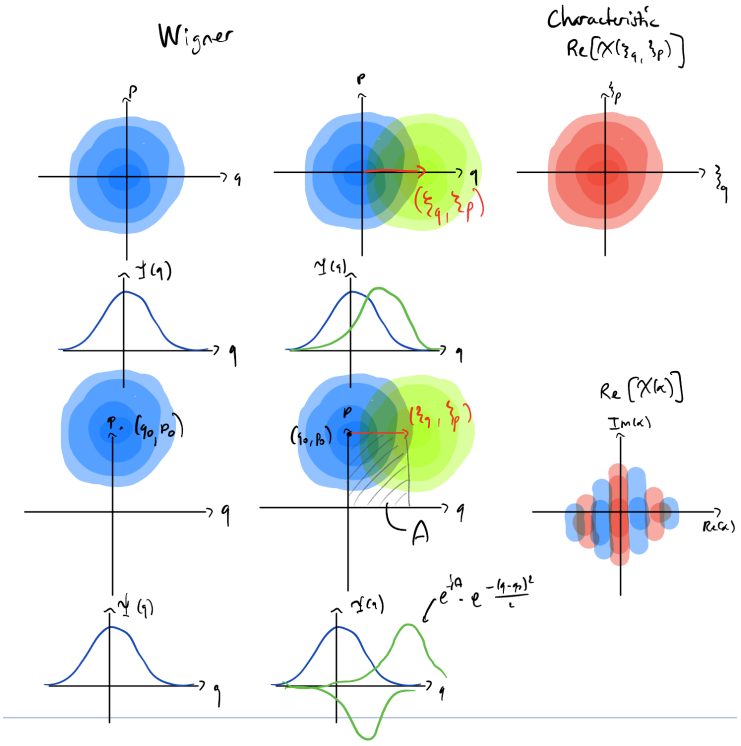

Figure 4: Sketch of the characteristic functions of a vacuum/ground state (top row) and of a displaced state (bottom row). The wavefunctions below show the overlap.

Consider now a displaced state $|\alpha\rangle$, shown on figure 4 in the second row. To calculate χ we must compare a state and its displaced self. The geometric phase now comes into play

$$\begin{aligned}
\chi(\xi_q,\xi_p)_\alpha &= \langle\alpha|\,\hat{D}(\xi_q,\xi_p)\,|\alpha\rangle \\
&= \langle 0|\,\hat{D}^\dagger(\alpha)\hat{D}(\xi_q,\xi_p)\hat{D}(\alpha)\,|0\rangle \\
\text{Using } \alpha &= \tfrac{1}{\sqrt{2}}(q_0+ip_0) \\
&= \langle 0|\,\hat{D}^\dagger(q_0,p_0)\hat{D}(\xi_q,\xi_p)\hat{D}(q_0,p_0)\,|0\rangle \\
&= \langle 0|\,\hat{D}^\dagger(q_0,p_0)\hat{D}(q_0,p_0)\hat{D}(\xi_q,\xi_p)e^{-i(\xi_q p_0-\xi_p q_0)}\,|0\rangle \\
&= \langle 0|\,\hat{D}(\xi_q,\xi_p)\,|0\rangle\, e^{-iA} \\
&= \langle 0|\,\hat{D}(\xi_q,\xi_p)\,|0\rangle\, e^{-iA} \\
&= e^{-(\xi_q^2+\xi_p^2)/4}e^{-iA}
\end{aligned}$$

with $A=\xi_q p_0-\xi_p q_0$. On figure 4 in the second row is shown how an initially

displaced state acquires this phase, and how the characteristic function looks like schematically (bottom right). The accumulated phase grows with the area, such that a state that is further out displaced will display faster oscillations.

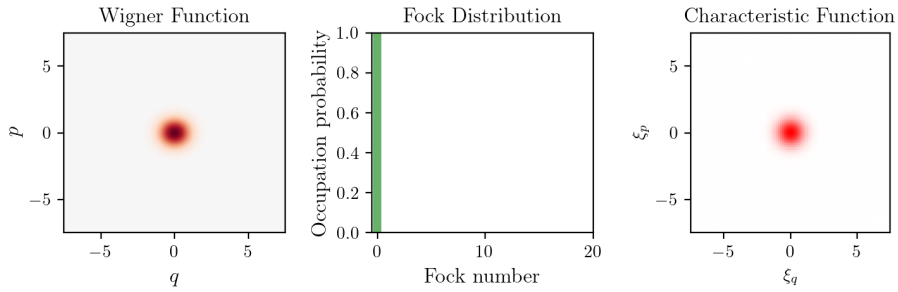

Figure 5: Ground state

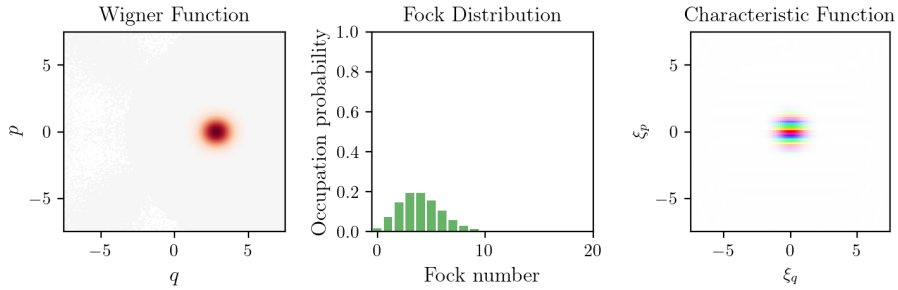

Figure 6: Displaced state with $\alpha = 2$. The colors in the characteristic function represent phase, and the intensity the magnitude.

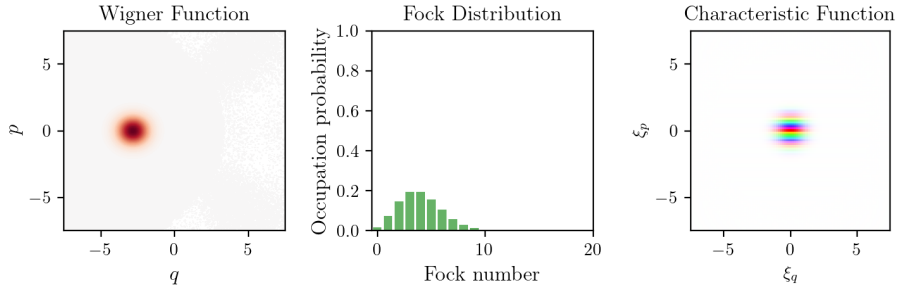

Figure 7: Displaced state with $\alpha = -2$. Notice the phase pattern in the characteristic function is inverted.

Squeezed states The squeezing operator is defined as

$$\hat{S}(r) = e^{\frac{1}{2}(\hat{a}^2\xi^* - \xi(\hat{a}^\dagger)^2)}$$

and recall that its action on the quadratures for $\xi = r \in \mathbb{R}$

$$\hat{q} \to \hat{q}e^{-r}, \quad \hat{p} \to \hat{p}e^{r}.$$

This is a rescaling the axes in phase space, such that we can guess that the function is indeed the squeezed state shown on figure 8.

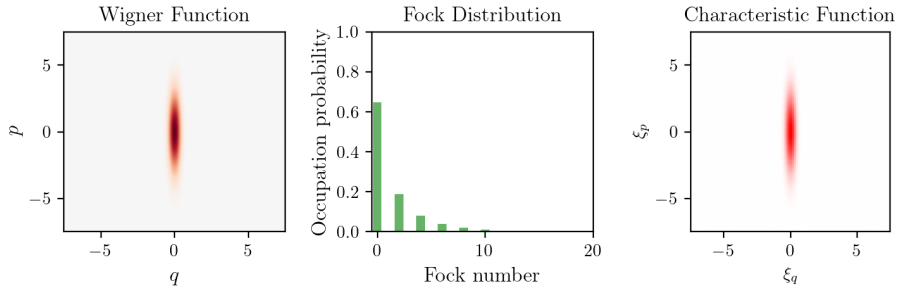

Figure 8: Squeezed state with $r = 1$

One can also turn the squeezing axis, see figure 9, or displace the squeezed state, figure 10. One can also squeeze along another direction, given the argument of ξ,

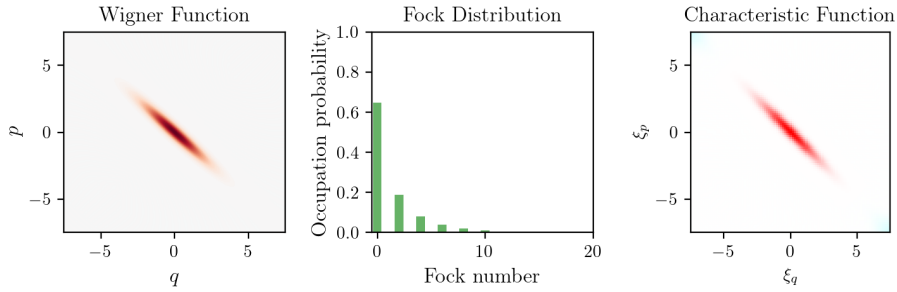

Figure 9: Squeezed vacuum with $\xi = i$

Displacing the squeezed state yields the interference pattern that we are familiar with from the displaced state, shown on figure 10

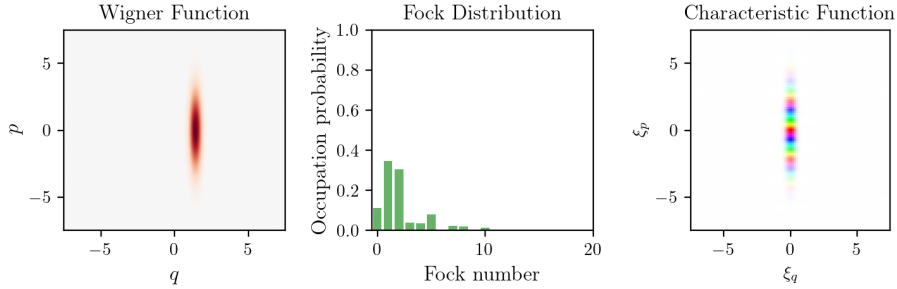

Figure 10: $\psi = \hat{D}(1)\hat{S}(1)\,|0\rangle$

Finally, what happens if a squeezed state loses a photon? Recall that the squeezed state only had even Fock states and thus even parity. Applying the lowering operator $\hat{a}$ hence changes the parity and we now have only odd Fock states. This means the Wigner function must be negative at the center, as shown on figure 11.

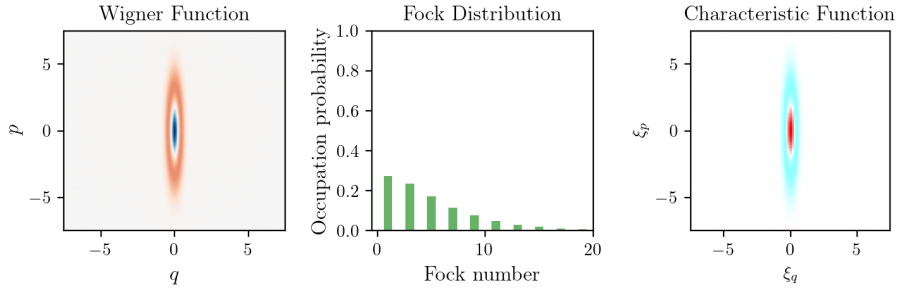

Figure 11: Squeezed state that lost exactly one photon, $|\psi\rangle \propto \hat{a}\hat{S}(r)\,|0\rangle$

Superposition states and mixed states Consider now a cat state, $|\psi\rangle \propto |\alpha\rangle + |-\alpha\rangle$. It is an even state, such that the Wigner function should be high in the center. Also, it is symmetric, such that the characteristic function is real. Wigner and χ are shown on figure 12. Notice that both look very similar. In the Wigner function, both lobes of the cat appear, with interference fringes between them being a signature of quantum coherence. In the characteristic function however, the lobes are the sign of coherence and the fringes are the signature of displacement.

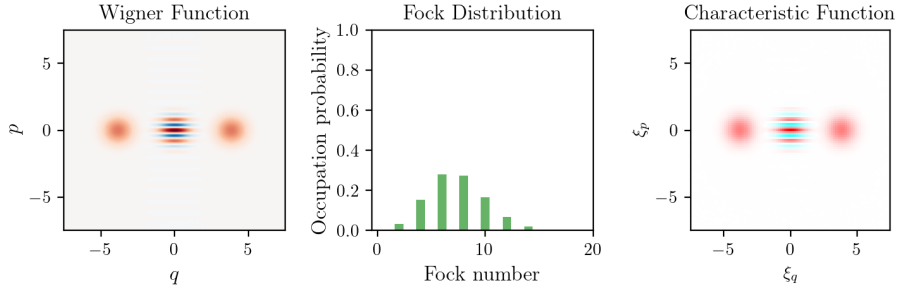

Figure 12: Even cat state $\propto |\alpha\rangle + |-\alpha\rangle$ with $\alpha = 2$

What happens if a cat state loses a phot(n)on? Applying the lowering operator gives us

$$\hat{a}(|\alpha\rangle + |-\alpha\rangle) = \alpha(|\alpha\rangle - |-\alpha\rangle)$$

This new state is now an odd cat state $|\psi\rangle \propto |\alpha\rangle - |-\alpha\rangle$. It has negative parity (-1), hence the Wigner function's fringes are inverted, and so are χ's lobes (now negative). See figure 13

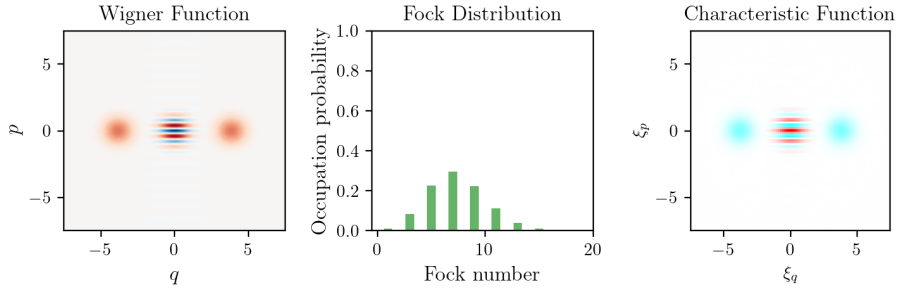

Figure 13: Odd cat state $\propto |\alpha\rangle - |-\alpha\rangle$ with $\alpha = 2$

The mixed state $\rho = \frac{1}{2}(|\alpha\rangle\langle\alpha| + |-\alpha\rangle\langle-\alpha|)$'s representations are shown on figure 14. It is essentially a statistical mixture between the odd and the even cat state. The signatures of coherence (fringes in Wigner, lobes in χ) are gone.

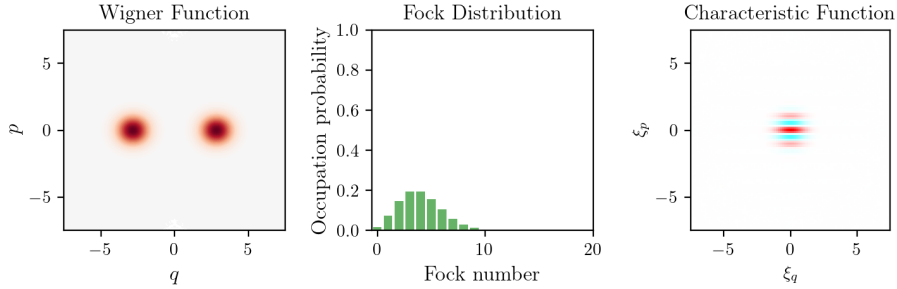

Figure 14: Mixed cat state $\rho = \frac{1}{2}(|\alpha\rangle\langle\alpha| + |-\alpha\rangle\langle-\alpha|)$

Fock states Fock states have no phase information (in the sense that neither q nor p are "preferred"), such that there is a circular symmetry in Fock states. This can be seen in their Wigner as well as χ functions, shown for $n = 1, 2$ on figures 15 and 16.

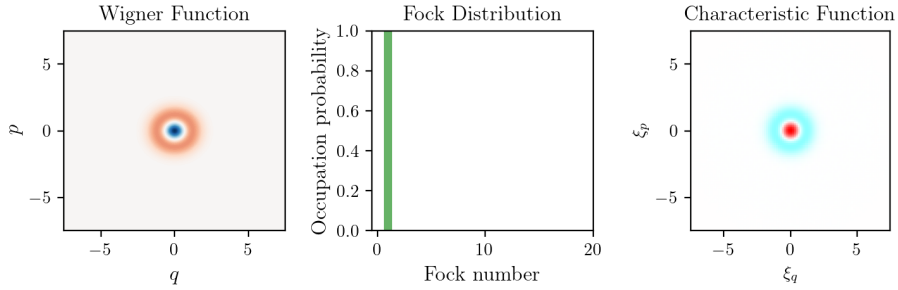

Figure 15: Fock 1 state

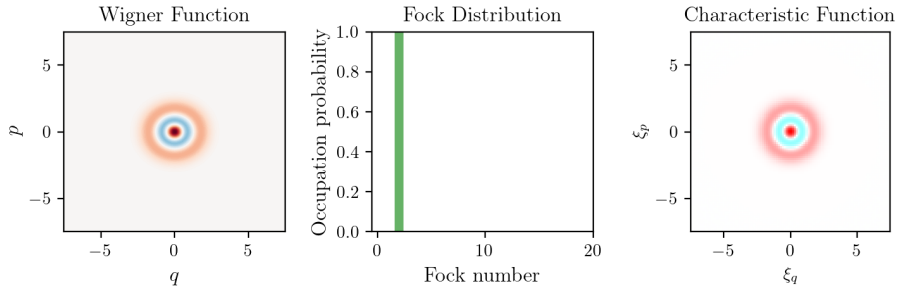

Figure 16: Fock 2 state

GKP States Finally, as an appetizer, we show the Wigner and characteristic function of the GKP (grid state). We will discover it further down in the lecture,

but can you guess what its constituents are?

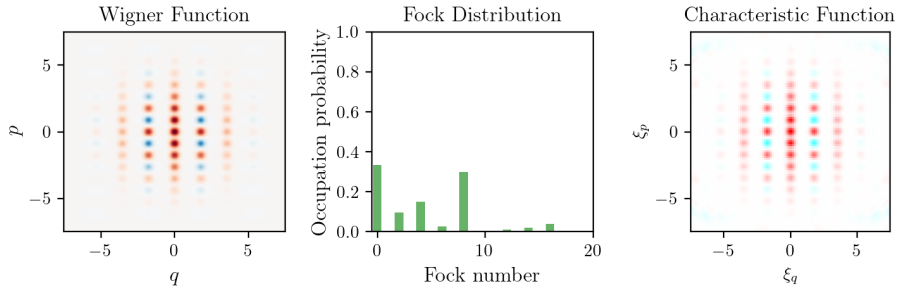

Figure 17: GKP logical $|0\rangle_L$

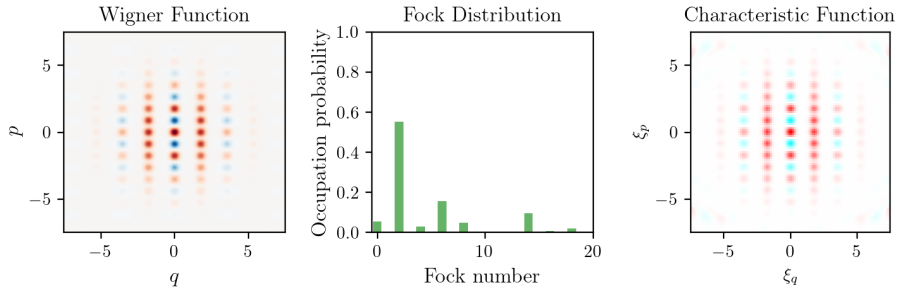

Figure 18: GKP logical $|1\rangle_L$

5 The Trapped Ion Toolbox

Trapped ions are a leading platform for quantum optics and quantum information experiments, as they are a quantum system that is identically reproduceable, extremely well isolated, and easily manipulatabled. In "standard" trapped ion quantum information, the information (qubit) is encoded in well chosen electronic levels of the ion, and using these the best single-qubit and two-qubit gates (at time of writing) have been demonstrated, and arguably the deepest quantum circuits have been run. They also allow probing fundamental physical constants and can be used for atomic clocks. Of particular relevance to this lecture, a trapped ion's motion is extremely well described by a harmonic oscillator. Additionally, ions are charged, allowing for an efficient mediation of interactions using the Coulomb force. We will explore their properties and see how one can write, manipulate and read out quantum information in the motion of a trapped ion.

Before starting, however, it is advisable to take a step back. A common motivation for encoding qubits into an oscillator is that one can leverage the additional

redundancy of the larger Hilbert space in order to accommodate an error correcting code, thus improving the qubit. Trapped ions are, however, already excellent qubits. By choosing the electronic levels and the right species, one has access to a qubit with effectively infinite T1 and clock-limited T2. We call these levels clock transitions, as they are used to make atomic clocks. (i.e. the timekeeping ability "clock" of the ion is often better than the control system clock, hence the T2 limit). Essentially, ions, if well-trapped and taken care of, are already perfect qubits. Rather, the difficulty lies in creating gates that operate without fault.

Here again, the standards are excruciatingly high. The highest fidelity two-qubit gate ever reported has been done in a pair of two trapped ions (Oxford group/Oxford Ionics). However, since the gates are mediated through the oscillator's degree of freedom, there could be room for improvement using bosonic qubits. Faults happening during a gate operation could be caught and corrected if the mediating oscillator uses a bosonic, redundant encoding.

On a different level, operating a clock qubit requires being at a very specific magnetic field and use very specific transitions, setting stringent experimental constraints on geometry and lasers used. Using the bosonic qubits written into the motion of the ion could alleviate the requirements, allowing for a more noisy platform, more experimental flexibility and make the general architecture more versatile.

Looking at different quantum computing platforms, trapped ions and neutral atoms are very similar, and tools used in one platform can often be similarly transferred to the other, so there is value to study the trapped ion case and potentially transfer ideas from ions to neutral atoms. One caveat is that the oscillators available in neutral atoms are rarely linear as the optical tweezer used to trap them is typically orders of magnitude less harmonic than typical ion traps.

Another route towards bosonic quantum information processing that could be imagined involves photonics. It is very hard to create non-Gaussian states in a photonic platform, and here a trapped ion could be used to transduce the non-Gaussian phonons to photons. This is early work though, currently hindered by collection efficiency and light-ion coupling.

Finally, one does not always need a plan. Many scientific discoveries were not "planned", rather fortunate accidents. There are many things to learn from trying things!

With these things said, it is time to dive into the business of writing bosonic qubits into ions.

5.1 Trapping & Normal Modes of Trapped Ions

It is impossible to trap a charged particle with static electric fields alone (ions we use are typically positive). Indeed, it would mean that all electric field

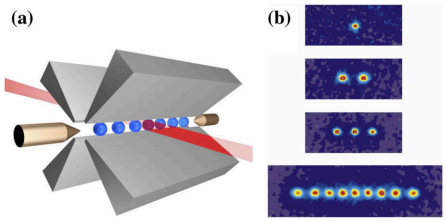

Figure 19: Paul trap. Figure courtesy of University of Innsbruck. **a)** A typical "blade" trap. Two opposing blades are the RF electrodes, generating an oscillating saddle potential. The two other blades are DC-electrodes, providing control over the motional modes. Finally, end-cap electrodes ensure the trapped ions remain in the center of the trap. **b)** Ion crystals in a Paul trap. One of the directions is much less confining than the others, such that the positively charged ions arrange along this direction (axial direction).

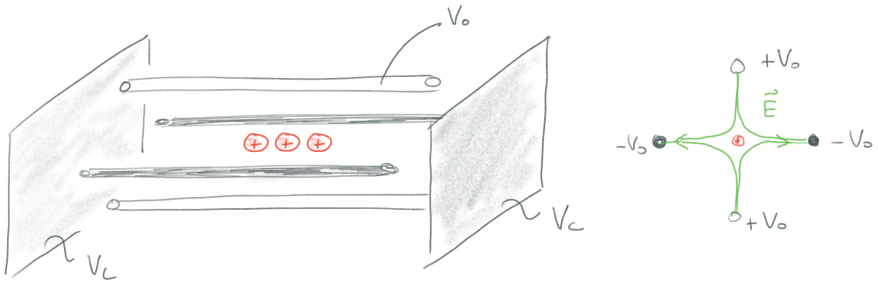

Figure 20: A typical Paul trap. Two opposing rods are the RF electrodes (voltage V_0), generating an oscillating saddle potential. The two other blades are DC-electrodes, providing control over the motional modes. Finally, end-cap electrodes ensure the trapped ions remain in the center of the trap (voltage V_c).

lines point towards a certain region of space, which by Gauss's law implies the presence of an opposite charge at the trapping location. So how do you even trap an ion?

5.1.1 The Paul trap

The main idea is to put four rods/electrodes in a configuration such as shown on figure 20. When applying a voltage to the electrodes, the electric potential at the center of the trap can be written as

$$V(x,y,z) = \underbrace{\frac{V_0}{r_0^2}(x^2-y^2)}_{\text{rods}} + \underbrace{\frac{V_c}{r_c^2}(2z^2-x^2-y^2)}_{\text{end-caps}}$$

where r_0 and r_c are geometric parameters, V_0 the voltage applied on the rods and V_c the voltage applied onto the end-caps. This potential satisfies Laplace's

equation, $\Delta V_C = 0$ and on its own will not trap. The trick to make it trapping is to use a quickly (quicker than the ion's motion) alternating voltage on the rods,

$$V_0 \to V_0 \cos(\Omega_{\mathrm{RF}} t),$$

exerting a so-called ponderomotive force, which creates an effective trapping potential. In the following, we will explore in the 1D case how the ponderomotive force allows us to trap ions. For that, we want to solve the equation of motion for the trapped ion's position x. We assume it is in an electric potential $V(x,t) = V(x)\cos(\Omega_{\mathrm{RF}} t)$ and has charge q and mass m. The electric force $f(x)$ is given by taking the gradient of the potential,

$$f(x) = -qV'(x)$$

such that we can write an equation of motion

$$m\ddot{x} = F = f(x)\cos(\Omega_{\mathrm{RF}} t)$$

We assume that the ion's motion is on a slower timescale than $1/\Omega_{\mathrm{RF}}$, and separate the timescales of movement into a slow and a fast oscillation

$$x(t) = \underbrace{X(t)}_{\text{slow}} + \underbrace{\xi(t)}_{\text{fast}}$$

expanding the force around the position X

$$f(x) = f(X+\xi) = f(X) + \xi f'(X) + \mathcal{O}(\xi^2)$$

we separate the slow and fast dynamics. We do two assumptions: First, we assume that $\xi f'(X) \ll f(X)$, and that the timescale of X is much slower than $2\pi/\Omega_{\mathrm{RF}}$. This enables us to also separate the equation of motion, in which the fast dynamics then satisfy

$$m\ddot{\xi} = f(X)\cos(\Omega_{\mathrm{RF}} t)$$

to first order. Integrating we get

$$\xi(t) = \frac{-f(X)}{m\Omega_{\mathrm{RF}}^2}\cos(\Omega_{\mathrm{RF}} t)$$

and we can substitute this back into the main equation to solve for X

$$m\ddot{x} = m(\ddot{X} + \ddot{\xi}) = f(X+\xi)\cos(\Omega_{\mathrm{RF}} t)$$

we take the time-average over $t = 2\pi/\Omega_{\mathrm{RF}}$ denoted by $\langle\cdot\rangle$. Since $\langle\xi\rangle = 0$, and $\langle X\rangle = X$ we have

$$m\ddot{X} = \langle f(X+\xi)\cos(\Omega_{\mathrm{RF}}t)\rangle \approx \langle (f(X) + \xi f'(X))\cos(\Omega_{\mathrm{RF}}t)\rangle \tag{1}$$

$$= \underbrace{\langle f(X)\cos(\Omega_{\mathrm{RF}}t))\rangle}_{=0} + \frac{-f(X)f'(X)}{m\Omega_{\mathrm{RF}}^2}\underbrace{\langle\cos^2(\Omega_{\mathrm{RF}}t))\rangle}_{=1/2} \tag{2}$$

$$= -\frac{f(X)f'(X)}{2m\Omega_{\mathrm{RF}}^2} \tag{3}$$

$$= -\frac{d}{dX}\left[\frac{f(X)^2}{4m\Omega_{\mathrm{RF}}^2}\right] = \boxed{-\frac{d}{dX}\Phi(X)} \tag{4}$$

with $\Phi(x)$ being the ponderomotive potential. It generalizes to 3D where the confining potential is simply proportional to the electric field's norm squared,

$$\Phi(x,y,z) = \frac{q^2|\vec{E}(x,y,z)|^2}{4m\Omega_{\mathrm{RF}}^2}$$

which in the case of our quadrupole field stemming from the rods then gives a potential $V_{RF} \propto x^2 + y^2$. While the oscillating electric potential V_0 ($\vec{\nabla}V_0 = \vec{E}(x,y,z)$) has to satisfy Laplace's equation at all times (and cannot be completely confining), this new effective potential scales like $V_{RF} \sim |\vec{E}|^2$ which does not satisfy Laplace's equation anymore, and can be completely confining.

Note that this derivation assumes $\xi \ll X$, which is typically the case in most Paul traps. In the trapped-ion community, we call ξ the micromotion and X the secular motion of the ion. When this assumption is not satisfied, one has to resort to solve the Mathieu equation, and several stability regimes appear. For more details, I recommend looking at *Exploring the Quantum* (Haroche / Raymond).

To better understand the trapping effect, a few comments are in order:

First, in a very mechanical interpretation, the micromotion is such that during a period, when the potential is confining, the ion is further away from the center than when it is anti-confining, figure 21. On average, the ion thus gets pushed more in than out, thus creating an average trapping potential.

Second, the further out the ion is, the more micromotion it experiences, and hence the more kinetic energy it has. The slow motion experiences this kinetic energy as a potential, and the ion will be pushed back to the center of the trap, minimizing micromotion.

Finally, there is a direct analogy with optical tweezers and the AC stark shift. In optical tweezers, a repulsive force can be created by driving a beam blue-detuned of a transition in this atom. The light induces a dipole moment in the atom, which is out of phase with the light, and thus the light exerts a repulsive force on the ion, pushing it out of the high-intensity region. The ion

Figure 21: The micromotion is such that when the ion is at its maximal point, it gets pushed back in maximally.

can be thought of as having an effective polarizability, as when it is excited by an electric field it starts oscillating and thus creates a dipole[1]. Similarly to the blue-detuned beam, the dipole created by the oscillating ion will be expelled from the high-field regions (in this case it will go to the center of the trap). It's the same physics, with the main difference being that in the atom case the induced dipole is intrinsic to the atom (it's the orbitals), while in the ion's case there is an effective dipole due to the oscillation ξ induced by the trapping potential.

To operate the trap, we then combine the oscillating field with a static one, and we obtain a confining potential

$$V(x,y,z) = \frac{q^2 V_0^2}{m\Omega_{\mathrm{RF}}^2 r_0^4}(x^2+y^2) + \frac{V_c}{r_c^2}(2z^2 - x^2 - y^2),$$

for appropriately chosen values of V_0 and Ω_{RF}. More recent traps are composed out of segmented electrodes, allowing a more flexible tuning of the DC components, such that we can write

$$V(x,y,z) = \frac{q^2 V_0^2}{m\Omega_{\mathrm{RF}}^2 r_0^4}(x^2+y^2) + \frac{V_c}{r_c^2}(\alpha x^2 + \beta y^2 + \gamma z^2),$$

where $\alpha + \beta + \gamma = 0$ are the DC components and satisfy the Laplace equation. Such a trap is shown on figure 23.

Now coming back to bosonic quantum information, Paul traps form (very) harmonic potentials along three spatial dimensions, giving rise to a 3D quantum harmonic oscillator with three normal motional modes. This allows us to write out a Hamiltonian for the motion of a trapped ion as

$$H_m = \sum_{i=1}^{3} \hbar\omega_i \hat{a}_i^\dagger \hat{a}_i \tag{5}$$

with $\hat{a}_i$ the ladder operators associated to the normal mode i. Typically frequencies of the modes range from 0.2 to 5 MHz. Interestingly, the motional frequency stability is directly related to how stable the electric fields trapping

[1]The polarizability of a free charge of mass m and charge q is $\frac{q^2}{2m\Omega^2}$

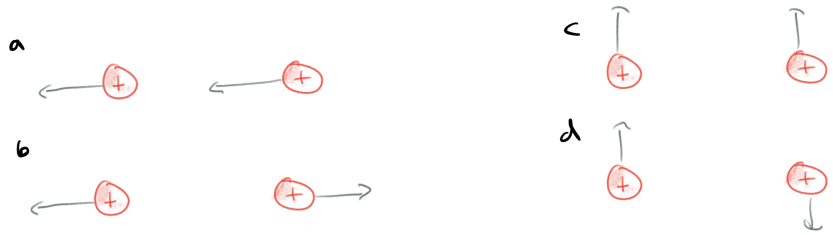

Figure 22: Different eigenmodes for a two-ion crystal. **a** The COM mode at ω_z the axial frequency. **b** the stretch/breathing mode at $\sqrt{3}\omega_z$. **c** Radial COM mode at frequency ω_x **d** Radial stretch mode at frequency $\sqrt{\omega_x^2 - \omega_z^2}$

it are. Hence if one engineers a system that is stable enough, one can expect good oscillator coherence times ($\sim$ 40 ms at 2 MHz).

A natural question to ask is what happens when more than one ion is in the trap. Ions interact through the Coulomb force, repelling each other. The typical regime in which ion traps operate is where one of the directions is much less confining than the two other directions. In that regime the ions will arrange along a line, forming a one-dimensional ion crystal. This is particularly interesting in the context of this lecture because now they are not acting as spatially local oscillators, but rather share a collective motion. The fundamental axial mode consists of all ions moving collectively along the same direction and with the same phase. In the case of two ions, there are also rocking modes and stretch modes, see figure 22. This generalizes with N ions, where the crystal possesses $3N$ modes.

These shared, quantized, motional degrees of freedom can be used as a bus to mediate interactions between internal levels of the different ions. By far the highest fidelity two-qubit gates in quantum information processing have been mediated by using the motional modes of an ion crystal.

Note that there is another architecture for ion traps called Penning traps, where the oscillating potential's confining role is replaced with a strong magnetic field, the Lorentz force creating circular trajectories along which the ion precess. You can learn more about them in Daniel Kienzler's lecture on trapped ion physics.

5.2 Internal degrees of freedom

Before we can start with bosonic information processing, we need to discuss the specifics of ions. The trapped species[2] typically is alkaline-earth. Alkaline-earth elements are found in the second column of the periodic table and posses two valence electrons when neutral. In experiments, the atom is *ionized*, that is one electron is ejected from its orbit, leaving a single valence electron orbiting the

[2]element trapped, e.g. Calcium (jargon)

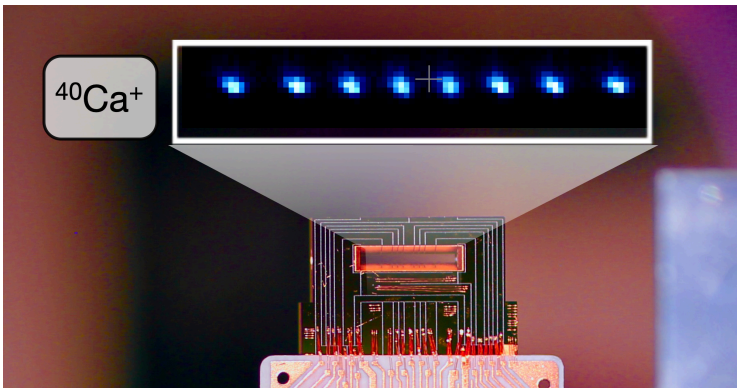

Figure 23: The GKP ion trap at TIQI/ETH Zürich. The trap is 10mm from edge to edge. The inter-ion distance is approximately 10 µm. Wirebonds connect the trap's electrodes to a PCB, through which the electrical signals to control the trapping potentials are routed. Instead of four rods and two end-caps we have here 22 individually addressable electrodes, allowing us to create non-trivial potentials. The ions are spaced by ∼10 µm, while the trap is approximately 1 cm in length.

nucleus and inner electrons. Alkaline-earth species thus provide singly charged ions with a relatively simple electronic structure due to the fact that there is a single valence electron. The inner core electrons fill all the core shells and their transitions are in the EUV/X-Ray range, such that the valence electron doesn't interact with them. In the lab, ionization is typically achieved using a combination of laser pulses pointed into an atomic beam flying through the trap. In this way we can ionize the atom in the center of the trap and catch it.

We are now interested in the energy-level structure of the ion. As you know from quantum mechanics, the electron is bound in orbitals that have different eigenenergies. Before we go into details, it is good to think about properties of the orbitals. There are typically three categories of orbitals. First, ground states. Ground states are the lowest energy levels and hence have "infinite" lifetime. Atomic clocks often rely on ground-state manifolds. Then, there are long-lived (1 s-100 s) metastable states that are typically well seperated in energy from the ground state (100-1000 THz) but still long-lived. They are useful for quantum information processing, as transitions between ground and metastable states can be driven using lasers and have very long coherence times. Finally, there are short-lived states (10s of ns or less), which also fluoresce (emit light) when decaying. They are useful for readout, where a transition between a long-lived and a short-lived state is driven, emitting many photons that can be then detected on a photomultiplier tube or a camera. When one shows pictures of ions, typically a short-lived transition is driven to reveal them (23).

Let's take $^{40}Ca^{+}$ as an example. We have a ground state that the ion naturally

relaxes to. Then, there is a short-lived (10s of ns) P-orbital manifold. Finally, there are two metastable orbitals (D5/2 and D3/2) that can be used to store information. Typically, 4S1/2 $\leftrightarrow$ 3D5/2 is used as a qubit[3]. Figure 24 shows the energy level structure.

For practical purposes, it is sufficient to consider simply one long-lived transition, such that we can write a two-level Hamiltonian of the usual spin form

$$\hat{H}_{el} = \hbar\omega_{eg}\frac{\hat{\sigma}_z}{2} = \frac{\hbar\omega_{eg}}{2}[|\uparrow\rangle\langle\uparrow| - |\downarrow\rangle\langle\downarrow|] \tag{6}$$

To prepare a $|\downarrow\rangle$ (4S1/2) state, we can drive a repumping transition using a laser at 854 nm that will excite the $|\uparrow\rangle$ (3D5/2) state to the P3/2 manifold, from where it will decay into the ground state.

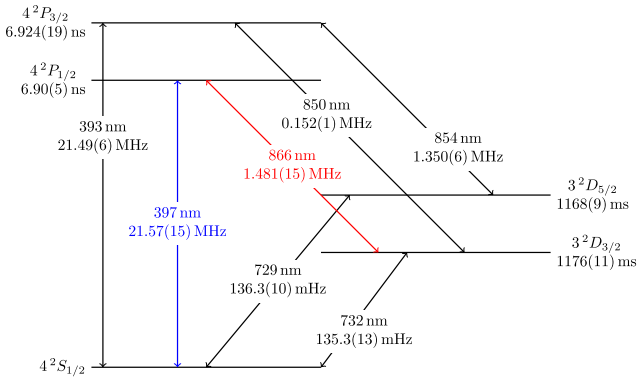

Figure 24: $^{40}Ca^+$ ion level scheme. From the ion trapping periodic table, `https://mike.depalatis.net/ionptable/calcium/`

5.3 Light-matter interaction

When one shines a laser onto a trapped ion, it sees an electric field $E(\vec{r},t) \propto E_+ \exp(i(\vec{k}\cdot\vec{r} - \omega_l t))$. Even though we work in the dipole approximation, that is, the emitter is much smaller than the wavelength, the emitter's position may probe different locations of the electromagnetic wave. This position-dependent light coupling allows coupling not only the internal degrees of freedom of the ion with electromagnetic radiation, but the motional degrees of freedom as well (i.e. its position) in a fashion that is similar to the previously seen optomechanics. Let's reveal the math behind this.

When writing out the interaction Hamiltonian of an ion in a propagating light

[3]We omit the fine structure here

field we now have to take into account its position $\hat{r} = (\hat{x}, \hat{y}, \hat{z})^\top$ in

$$\hat{H}_{int} = -\frac{i\hbar\Omega}{2}\hat{\sigma}_+ e^{i(\vec{k}\hat{r}-\omega_l t)} + \text{h.c.}, \tag{7}$$

where $\hat{\sigma}_+ = |e\rangle\langle g|$ and Ω the Rabi frequency. It is useful to go into a rotating frame using $U(t) = \exp(i\omega_{eg}\hat{\sigma}_z t/2)$[4] such that

$$\hat{H}_{int} \xrightarrow{\text{rotating frame}} \hat{H}_{int} = -\frac{i\hbar\Omega}{2}\hat{\sigma}_+ e^{i(\vec{k}\hat{r}-\Delta t)} + \text{h.c.}, \tag{8}$$

with $\Delta = \omega_l - \omega_{eg}$. Now let's restrict ourselves to a single motional mode $\hat{x}$, which can be done if the modes are sufficiently separated in frequency and cold enough. We are interested in the term $\vec{k}\hat{x}$, where the ion's position appears. Writing it in terms of ladder operators we have

$$\vec{k}\hat{x}\vec{\epsilon}_x = |k|\cos(\theta)x_{\text{zpf}}(\hat{a}+\hat{a}^\dagger) = \eta(\hat{a}+\hat{a}^\dagger), \quad \eta = |k|x_{\text{zpf}}\cos(\theta) = \sqrt{\frac{\hbar k^2}{2m\omega_x}}\cos(\theta),$$

where $\vec{\epsilon}_x$ is the mode's orientation, θ being the angle between the wave-vector (direction of light propagation) and the mode orientation, $x_{\text{zpf}} = \sqrt{\hbar/(2m\omega_x)}$ the mode's ground state size/zero-point fluctuations. We introduced η, the Lamb-Dicke (LD) parameter, which can be interpreted in two ways.

Firstly, η is the ratio of the size of the ion's ground state wavepacket (≈ 10 nm) to the wavelength (729 nm) divided by 2π. If η is small, then the light field the atom sees is approximately linear on the scale of its position, hence we can linearize the light field (Figure 25). If the ion's position wavefunction is on the same length scale than the wavelength, different parts of it probe a different light field, creating a non-linear interaction. This is a first interpretation on how to understand the LD-parameter.

Secondly, it can be understood in terms of recoil energy of the transition. An elastic scattering event has recoil energy $E_r = \frac{\hbar^2 k^2}{2m}$ (by conservation of momentum). Notice that

$$\eta = \sqrt{\frac{E_r}{\hbar\omega_x}}$$

that is, the LD parameter is the square root of the ratio of recoil energy to quantization energy. This means η tells us how strongly a recoil photon at this transition can "kick" the oscillator.

Plugging in numbers, $\lambda = 729$ nm, $\omega_x \approx 2$ MHz and $m = 40$ amu, we find that

[4] It is implicit that $\hat{\sigma}_z = \hat{\sigma}_z \otimes \mathbf{1}_m$ where $\mathbf{1}_m$ is the identity operator on the oscillator's Fock space.

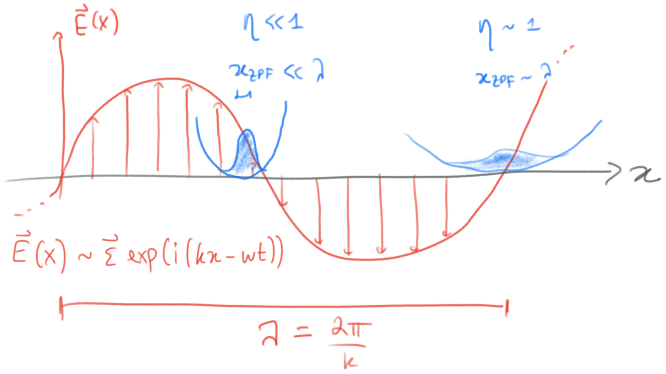

Figure 25: Interpretation of the Lamb-Dicke parameter

$\eta \sim 0.05 \ll 1$ such that we can perform the *Lamb-Dicke expansion*

$$H_{int} = -\frac{i\hbar\Omega}{2}\hat{\sigma}_+ e^{-i\Delta t}\left(1 + i\eta(\hat{a} + \hat{a}^\dagger) - \frac{\eta^2}{2}(\hat{a} + \hat{a}^\dagger)^2 + \mathcal{O}(\eta^3) + \text{h.c.}\right) \tag{9}$$

$$= -\frac{i\hbar\Omega}{2}\hat{\sigma}_+ e^{-i\Delta t}\left((1 - \eta^2(\hat{a}^\dagger\hat{a} + 1/2)) + i\eta(\hat{a} + \hat{a}^\dagger) - \frac{\eta^2}{2}(\hat{a}^2 + (\hat{a}^\dagger)^2) + \mathcal{O}(\eta^3) + \text{h.c.}\right) \tag{10}$$

This expansion now contains several terms. To understand their effect, we now once again go to a new rotating frame $U'(t) = \exp(i\omega_x \hat{a}^\dagger\hat{a}t)$, mapping $\hat{a} \to \hat{a}e^{-i\omega_x t}$. Tuning the laser frequency ω_l allows us to select terms by bringing them in or out of resonance. First, when $\Delta = 0$, we recover our usual carrier drive, although the Rabi frequency is slightly altered by the phonon occupation number[5].

$$H = \frac{\hbar\Omega(1 - \eta^2(2\hat{a}^\dagger\hat{a} + 1))}{2}\hat{\sigma}_y$$

here the terms in $\hat{a}\hat{\sigma}_\pm, \hat{a}^\dagger\hat{\sigma}_\pm$ have prefactor $\eta\Omega/2\exp(\pm i\Delta t)$, such that we can use the rotating wave approximation to approximate them away in the limit $\Omega\eta \ll \Delta$.

Secondly, there are the terms to first order in $\hat{a}$. If we choose $\Delta = -\omega_x$, that is, we are tuning the laser *red* of the electronic transition by one motional frequency i.e. driving the red sideband. After a rotating wave approximation (note here that we require $\Omega \ll \Delta$), the Hamiltonian is

$$H_{rsb} = \frac{\hbar\Omega\eta}{2}(\hat{\sigma}_+\hat{a} + \hat{\sigma}_-\hat{a}^\dagger) \tag{11}$$

[5]What happens when the phonons are in a thermal state?

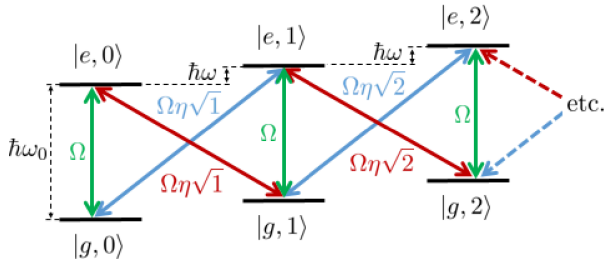

Figure 26: Sideband transitions. Taken from Daniel Kienzler's Trapped Ion lecture notes.

Notice the familiar Jaynes-Cummings form of the Hamiltonian[6]. Similarly, when $\Delta = \omega_x$, we can drive a blue sideband

$$H_{bsb} = \frac{\hbar\Omega\eta}{2}(\hat{\sigma}_+\hat{a}^\dagger + \hat{\sigma}_-\hat{a})$$

which is now an anti-Jaynes-Cummings Hamiltonian.

Figure 26 shows the energy levels of the spin-oscillator system. The red sideband transition excites the spin while removing a quanta of motion. On the other hand, the blue sideband transition both excites the motion and the spin.

Finally, second sideband transitions of the form can also be driven, but their coupling strengths are typically very weak in the Lamb-Dicke approximation.

$$H_{ssb} = i\frac{\hbar\Omega\eta^2}{4}(\hat{\sigma}_+\hat{a}^2 - \hat{\sigma}_-(\hat{a}^\dagger)^2)$$

Now, more complex interactions can be engineered by combining the above Hamiltonians. A workhorse of trapped-ion interactions is the bichromatic drive, where both a red and a blue sideband are driven simultaneously. When adding both one finds an interaction of the form

$$H_{rsb}+H_{bsb} = H_{sdf} = \frac{\hbar\Omega\eta}{2}\hat{(}\hat{a}(\hat{\sigma}_+ + \hat{\sigma}_-) + \hat{a}^\dagger(\hat{\sigma}_+ + \hat{\sigma}_-)) = \frac{\hbar\Omega\eta}{2}\hat{\sigma}_x(\hat{a}+\hat{a}^\dagger) = \frac{\hbar\Omega\eta}{\sqrt{2}}\hat{\sigma}_x\hat{q}$$

with $\sigma_x = \hat{\sigma}_+ + \hat{\sigma}_-$, which implements a force on the ion that depends on the (internal) spin state (state-dependent force, SDF). Notice that it is a force because it has a $\hat{q}$ term, which is simply a slope potential. In this case, the force's sign (direction) hence depends on the sign. The interaction can be understood as

[6]If you have trouble remembering which one sideband is which, the red sideband has less energy than the blue sideband. It's about light (red light has less energy than blue light). It's *not* that red = hot and blue = cold, in fact it's exactly the opposite.

The unitary associated to the Hamiltonian is

$$\hat{U}_{sdf} = \exp\left(-i\gamma\hat{\sigma}_x\hat{q}\right)$$

with $\gamma = \Omega\eta t$. It may either be interpreted as a displacement in phase space conditioned on the spin, $\hat{D}(-i\hat{\sigma}_x\gamma/\sqrt{2})$ or as a spin rotation dependent on the position, $\hat{R}_x(\theta\hat{q})$ with $\theta = 2\gamma$.

When the LD parameter is such that $\eta \sim 1$, the interaction becomes non-linear. This can be used to generate all kinds of interesting states, such as cat states.

5.4 Cooling and state preparation of a trapped ion

We now turn our attention to generating "interesting" quantum mechanical states in the motion of the ion. Before we can do this, we have to bring the ion to its motional ground state though. Ground-state cooling is typically achieved by first *doppler-cooling* the ion to a small thermal state, after which a sequence of sideband-cooling pulses are applied. The idea is to combine red-sideband pulses with repumping (resetting) the $|e\rangle$ state to the $|g\rangle$ state (e.g. using 854 nm light in Ca), essentially walking down the harmonic ladder through the cooling. The first pulses need to be shorter than the last pulses[7]. Figure 27 shows the process.

Regarding state preparation, that is the operation that maps the qubit from an unknown state $\hat{\rho}$ to a pure state $|\downarrow\rangle$, this can be done using a repumping sequence, in Ca using the 854 nm transition for example[8].

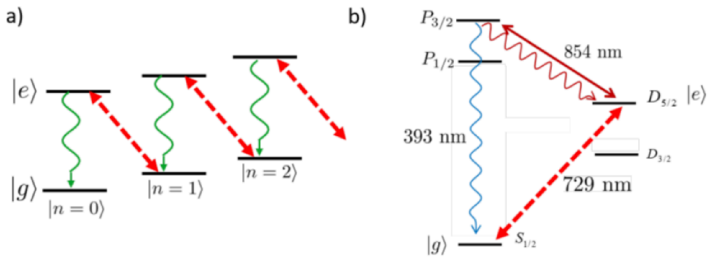

Figure 27: Sideband cooling an ion. The red sideband excites the spin degree of freedom from $|g\rangle$ to $|e\rangle$ while removing a quanta of motion. The spin is then brought back through a repump pulse, scattering only very few photons. Once the ground state is reached, the laser can no longer drive the transition and the state becomes "dark". Figure taken from Daniel Kienzler's lecture notes.

[7] Think about why!

[8] The details are a bit more complicated, see the specialized lecture on trapped ions

5.5 Gaussian operations in trapped ions

With this toolbox at hand, we can start examining which non-classical states we can prepare. We will go into more details in the exercises, so here we will give flavour of Gaussian operations can be generated. Displacements can be realized by driving an electric field that then couples to the charge of the ion

$$H_{int} = -qE(t)\hat{X}.$$

This interaction, when using an E field that is resonant with the ion's motional frequency, can be used to engineer the operator $\hat{D}(\alpha)$ (see exercises).

In the exercises we will also visit how to create the squeezing operator $\hat{S}(r)$. Squeezed states are useful for sensing, as they can reveal sub-Heisenberg limit displacements, and will be essential for GKP state preparation. Preparing a squeezed state is straightforward in an ion trap by modulating the trap strength k at twice the motional frequency $\omega_x = \sqrt{k/m}$:

$$H_{sq} = \frac{\hat{P}^2}{2m} + \frac{1}{2}(k_0 + k_1\cos(2\omega_x t))\hat{X}^2 \tag{12}$$

$$= \hbar\left[\omega_x + \frac{k_1}{k_0}\cos(2\omega_x t)\right]\hat{a}^\dagger\hat{a} + \hbar\omega_x\frac{k_1}{2k_0}\cos(2\omega_x t)(\hat{a}^2 + (\hat{a}^\dagger)^2) + \text{const.} \tag{13}$$

Looking at the interaction part we identify a squeezing Hamiltonian that generates the evolution

$$S(r) = \exp\left(-\frac{ir}{2}\left(\hat{a}^2 + (\hat{a}^\dagger)^2\right)\right)$$

Tuning the phase of the modulation allows to tune the squeezing angle.

5.6 Summary of possible interactions

Table 1 shows a list of possible interactions in trapped ions.

Interaction	Hamiltonian	Type of interaction
Displacement	$H = \hbar g(\hat{a} + \hat{a}^\dagger)$	Driven using electric fields
Squeezing	$H = \hbar g(\hat{a}^2 + (\hat{a}^\dagger)^2)$	Driven using electric fields
Red sideband	$H = \hbar\Omega\eta/2(\hat{a}\hat{\sigma}_+ + \hat{a}^\dagger\hat{\sigma}_-)$	Laser
Blue sideband	$H = \hbar\Omega\eta/2(\hat{a}\hat{\sigma}_- + \hat{a}^\dagger\hat{\sigma}_+)$	Laser
State-dependent force / Conditional displacement	$H = \hbar\Omega\eta/\sqrt{2}\hat{q}\hat{\sigma}_x$	Laser. Note: hard to realize without inducing significant spin dephasing
Tweezer	$H = \hbar I\hat{\sigma}_z\hat{n}$	Laser

Table 1: Summary of trapped ion native interactions

10 GKP codes: encoding qudits into grids

How can you encode a qubit into an oscillator? is the question Gottesman, Kitaev and Preskill set out to answer in 2001. The code they came up with is now known as the GKP code, and it was found to be the optimal way to encode, process and transmit information in a variety of different settings, with them sharing the fact that the main loss channels are simple creation and annihilation operators $\hat{a}, \hat{a}^\dagger$.

The way to construct the code is the following. Consider you have access to displacement operators of the harmonic oscillator, how would you create Pauli operators from it? A way to start is to look at the properties Paulis have to satisfy:

$$\hat{X}\hat{Z} = -\hat{Z}\hat{X}, \quad \hat{X}^2 = \hat{Z}^2 = \hat{I} \tag{14}$$

Our goal is to associate a Pauli algebra to displacement operators, i.e. we need to construct a set of displacement operators that behave in the same way a Pauli algebra does (equation 14). We will now associate a horizontal displacement (orange arrow below) to the operator $\hat{X}$ and a vertical displacement (blue arrow) to the operator $\hat{Z}$. As we saw previously, the area A between to paths starting and arriving at the same points in phase space gives their commutator, $\hat{X}\hat{Z} = e^{iA}\hat{Z}\hat{X}$. This means that in order to construct operators that anticommute $\hat{X}\hat{Z} = -\hat{Z}\hat{X}$, the paths need to enclose an area of π and their length should be $\sqrt{\pi}$. With that, we have satisfied the first of the two requirements.

We also need to satisfy that $\hat{X}^2$ is the identity. Recall the identity is such that $\mathbb{1}|\psi\rangle = |\psi\rangle$. If a translation is the identity, then it means the codewords must periodic in that displacement. We therefore impose a translational invariance

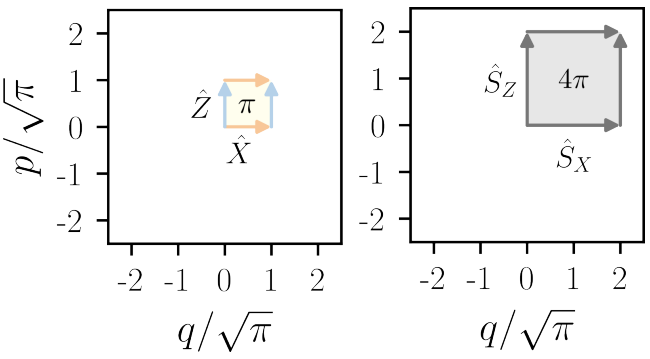

on the GKP codewords

$$|0\rangle_{GKP} \propto \sum_k |q = 2\sqrt{\pi}k\rangle\,, \quad |1\rangle_{GKP} \propto \sum_k |q = 2\sqrt{\pi}(k+\tfrac{1}{2})\rangle\,.$$

Along q, we therefore have an infite comb of δ functions around even/odd multiples of $2\sqrt{\pi}$. A sketch of the wavefunction is shown below.

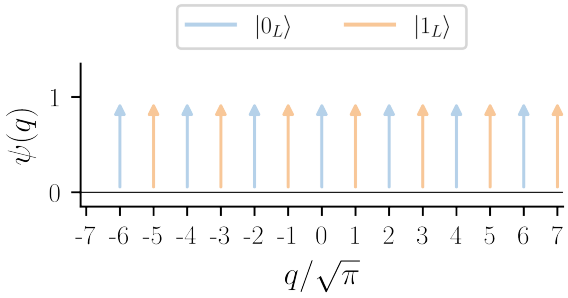

As we'll see later, these codewords satisfy the Pauli relations, i.e. $\hat{X}\,|0\rangle = |1\rangle\,, \hat{X}^2\,|0\rangle = |0\rangle$, but you can already see that translating the comb by $\sqrt{\pi}$ along q changes the $|0\rangle$ state to a $|1\rangle$ state. And going towards error correction, we can identify the stabilizers $\hat{S}_X = \hat{X}^2$, $\hat{S}_Z = Z^2$, the grid has a translational invariance. Below are shown the Wigner functions of these states. Notice that they are not only periodic along q, but also p, because they are linked through Fourier relations: if the wavefunction is periodic in q then it will also be periodic in p, with inverse frequency. One can see a grid ...!

This code is the most common GKP code, but it's not the only one. In order to keep it general, we are going to construct it in a way that generalizes to n modes and qu*d*its of dimension d (our example had $n = 1$ and $d = 2$, a single-mode qubit). For that we need to develop some mathematical machinery to deal with the n-mode phase space, which has a symplectic geometry (i.e. it's not a

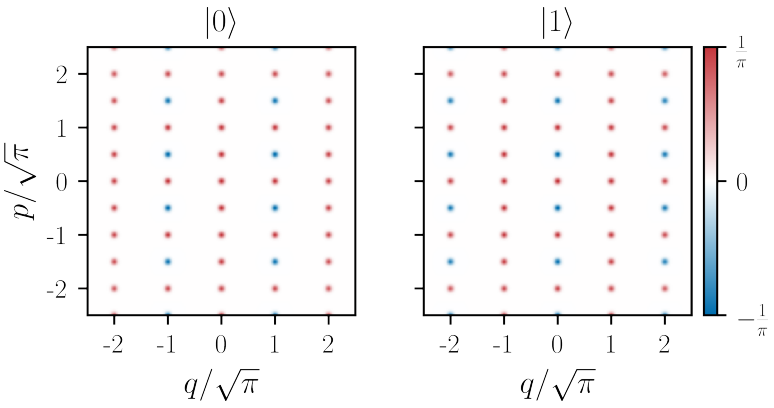

Euclidian space). Let's do this first. We will follow the formalism from Royer et al., *Encoding Qubits in Multimode Grid States*, PRX Quantum 3, 010335 (2022). This formalism is rather abstract, but I believe it to be worth the effort as it creates a structure that is very powerful and brings a lot of understanding as well as connections to other domains of QEC.

10.1 Basics of symplectic operations

Define the vector containing all quadrature operators of the n oscillators

$$\vec{x} = \begin{pmatrix} \hat{q}_1 \\ \hat{p}_1 \\ \hat{q}_2 \\ \hat{p}_2 \\ \dots \\ \hat{q}_n \\ \hat{p}_n \end{pmatrix}.$$

We then construct a matrix Ω encoding the commutation relations

$$[\hat{x}_j, \hat{x}_k] = i\Omega_{jk},$$

where $\hat{x}_j$ is the jth element of $\vec{x}$. For example, $[\hat{x}_1, \hat{x}_2] = [\hat{q}_1, \hat{p}_1] = i\Omega_{12} = i$.

Ω is given by

$$\Omega = \begin{pmatrix} 0 & 1 & 0 & 0 & \\ -1 & 0 & 0 & 0 & \dots \\ 0 & 0 & 0 & 1 & \\ 0 & 0 & -1 & 0 & \\ & \vdots & & & \ddots \end{pmatrix}.$$

Ω has three properties important for later: It is antisymmetric ($\Omega^\top = -\Omega$), it is orthogonal ($\Omega^\top\Omega = \mathbb{1}$), and it squares to minus the identity ($\Omega^2 = -\mathbb{1}$).

As we already saw, the GKP encoding requires treating displacement operators. Assume we want to displace the stace by a vector $\vec{u}$

$$\vec{u} = \begin{pmatrix} u_{q_1} \\ u_{p_1} \\ u_{q_2} \\ u_{p_2} \\ \dots \end{pmatrix}.$$

This operation (that we call $\hat{D}(\vec{u})$) needs to shift the quadrature vector

$$\hat{D} : \vec{x} \to \vec{x} + l\vec{u},$$

where l is a scaling factor that we'll need later. This is a displacement. $\hat{D}$ can be expressed as

$$\hat{D}(\vec{u}) = \exp\left(il\vec{x}^\top \Omega \vec{u}\right).$$

Proof

We assume w.l.o.g. $l = 1$. We want to prove that $\hat{D}^\dagger(\vec{u})\vec{x}\hat{D}(\vec{u}) = \vec{x} + \vec{u}$. Define the generator

$$\hat{A} \equiv \vec{x}^\top \Omega \vec{u} = \sum_{ij} \hat{x}_i \Omega_{ij} u_j, \qquad \hat{D}(\vec{u}) = e^{i\hat{A}}.$$

The Hadamard lemma (a corollary of the Baker–Campbell–Hausdorff formula) gives the conjugation of an operator by an exponential as

$$e^{-i\hat{A}}\hat{x}_k e^{i\hat{A}} = \hat{x}_k + [-i\hat{A}, \hat{x}_k] + \tfrac{1}{2}[i\hat{A}, [i\hat{A}, \hat{x}_k]] + \dots$$

such that we need to compute $[\hat{A}, \hat{x}_k]$. From the commutation relations $[\hat{x}_i, \hat{x}_j] = i\Omega_{ij}$,

$$[\hat{A}, \hat{x}_k] = \sum_{ij} \Omega_{ij} u_j [\hat{x}_i, \hat{x}_k] = i \sum_{ij} \Omega_{ij} \Omega_{ik} u_j = i \sum_j (\Omega^\top \Omega)_{jk} u_j = i u_k,$$

where we used $\Omega^\top \Omega = \mathbb{1}$. Since $[\hat{A}, \hat{x}_k] = iu_k$ is a number, $[\hat{A}, [\hat{A}, \hat{x}_k]] = 0$, and the Hadamard lemma terminates at first order:

$$\hat{D}^\dagger \hat{x}_k \hat{D} = e^{-i\hat{A}}\, \hat{x}_k\, e^{i\hat{A}} = \hat{x}_k + [-i\hat{A}, \hat{x}_k] = \hat{x}_k - i(iu_k) = \hat{x}_k + u_k.$$

Or, in vector form,

$$\hat{D}^\dagger(\vec{u})\vec{x}\hat{D}(\vec{u}) = \vec{x} + \vec{u}.$$

For the one-mode case, $\hat{D}$ has the familiar form

$$\hat{D}(\vec{u} \in \mathbb{R}^2) = \exp(i(u_p \hat{q} - u_q \hat{p})) = \hat{D}\left(\alpha = \tfrac{1}{\sqrt{2}}(u_q + i u_p) \in \mathbb{C}\right).$$

Now as alluded to previously we need to understand how different $\vec{T}$ commute. For $\vec{u}, \vec{v}$ we can write

$$\hat{D}(\vec{u})\hat{D}(\vec{v}) = e^{-il^2 \vec{u}^\top \Omega \vec{v}} \hat{D}(\vec{v})\hat{D}(\vec{u})$$

Proof

Again, for $l = 1$. Write the two displacements as $\hat{D}(\vec{u}) = e^{-i\hat{A}}$ and $\hat{D}(\vec{v}) = e^{-i\hat{B}}$ with generators

$$\hat{A} = \vec{x}^\top \Omega \vec{u}, \qquad \hat{B} = \vec{x}^\top \Omega \vec{v}.$$

Using the canonical commutation relations $[\hat{x}_i, \hat{x}_j] = i\Omega_{ij}$, the commutator of the two generators is

$$[\hat{A}, \hat{B}] = \sum_{ijkl} \Omega_{ij} u_j \Omega_{kl} v_l [\hat{x}_i, \hat{x}_k] = i \sum_{jl} u_j v_l \sum_{ik} \Omega_{ij} \Omega_{ik} \Omega_{kl}.$$

The inner sum over i reduces by orthogonality,

$$\sum_i \Omega_{ij} \Omega_{ik} = (\Omega^\top \Omega)_{jk} = \delta_{jk},$$

leaving

$$[\hat{A}, \hat{B}] = i \sum_{jl} u_j \Omega_{jl} v_l = i \vec{u}^\top \Omega \vec{v}.$$

This is a c-number: it commutes with both $\hat{A}$ and $\hat{B}$. The Baker–Campbell–Hausdorff formula therefore terminates after the first correction and gives

$$e^X e^Y = e^{X+Y} e^{\frac{1}{2}[X,Y]} \qquad \text{for } [X, Y] \in \mathbb{C}$$

Applying this to our two orderings,

$$\hat{D}(\vec{u})\hat{D}(\vec{v}) = e^{-i\hat{A}} e^{-i\hat{B}} = e^{-i(\hat{A}+\hat{B})} e^{-\frac{1}{2}[\hat{A},\hat{B}]} = e^{-i(\hat{A}+\hat{B})} e^{-\frac{i}{2}\vec{u}^\top \Omega \vec{v}},$$

$$\hat{D}(\vec{v})\hat{D}(\vec{u}) = e^{-i\hat{B}} e^{-i\hat{A}} = e^{-i(\hat{A}+\hat{B})} e^{-\frac{1}{2}[\hat{B},\hat{A}]} = e^{-i(\hat{A}+\hat{B})} e^{+\frac{i}{2}\vec{u}^\top \Omega \vec{v}}.$$

Such that

$$\hat{D}(\vec{u})\hat{D}(\vec{v}) = e^{-i\vec{u}^\top \Omega \vec{v}} \hat{D}(\vec{v})\hat{D}(\vec{u}) = e^{i\vec{v}^\top \Omega \vec{u}} \hat{D}(\vec{v})\hat{D}(\vec{u})$$

Note that from this proof one can also see that

$$\hat{D}(\vec{u})\hat{D}(\vec{v}) = \hat{D}(\vec{u} + \vec{v}) e^{-\frac{i}{2}\vec{u}^\top \Omega \vec{v}}.$$

The quantity $\vec{u}^\top \Omega \vec{v}$ has a geometrical interpretation, indeed it amounts to the oriented area in-between the vector $\vec{u}$ and $\vec{v}$, similarly to what we have seen in previous lectures, but now generalized to $2n$ dimensions. This is the machinery we needed.

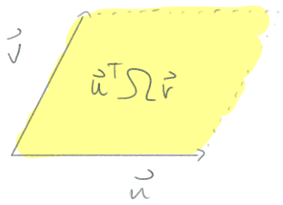

10.2 Constructing a code: Stabilizers and valid operations

Now let's entertain the idea of constructing a stabilizer group out of displacements.

Recall that the stabilizer group $\mathcal{S}$ and its codewords are defined by two properties. First, we have that all stabilizer operators commute with each other, i.e.

$$\mathcal{S} = \{\hat{S}_k : [\hat{S}_i, \hat{S}_j] = 0 \quad \forall \quad \hat{S}_i, \hat{S}_j\} \tag{15}$$

Then, codewords must satisfy

$$\hat{S}_k \left|\psi\right\rangle = \left|\psi\right\rangle \tag{16}$$

Constructing the stabilizer group $\mathcal{S}$ out of translation operators means we first have to satisfy equation 15. In particular, we will be looking for a set of vectors $\{\vec{s}_1, \vec{s}_2, ...\}$ that define a set of translation operators generating $\mathcal{S}$

$$\mathcal{S} = \{\hat{D}(\vec{s}_i) : i \in \{1, 2, ..., 2n\}\}.$$

Imposing that all elements of $\mathcal{S}$ commute amounts to

$$\vec{s}_i^{\top} \Omega \vec{s}_j = \frac{2\pi k}{l^2} \quad \forall \quad i, j, \quad k \in \mathbb{Z}. \tag{17}$$

This follows from the previously shown relation

$$\hat{D}(\vec{s}_i)\hat{D}(\vec{s}_j) = \hat{D}(\vec{s}_j)\hat{D}(\vec{s}_i)e^{il^2 s_i^{\top}\Omega s_j} \equiv \hat{D}(\vec{s}_j)\hat{D}(\vec{s}_i).$$

It now becomes useful to choose $l = \sqrt{2\pi}$, which will be used for the rest of this lecture. In these units, any pair of stabilizer operators must have displacement vectors forming a parallelogram in $2n$ dimensions of integer area $(..., -1, 0, 1, 2, ...)$. What now remains is finding the codewords. Codewords $\mathcal{C}$ are such that they are eigenstates of all stabilizer operators, i.e.

$$\mathcal{C} = \{\left|\psi\right\rangle : \hat{D}(\vec{s}_i)\left|\psi\right\rangle = \left|\psi\right\rangle, \forall i\} \tag{18}$$

It now becomes apparent why GKP states are referred to as grid states. Indeed, equation 18 imposes that all states are identical under translation by any $\vec{s}_i$.

This is exactly a grid! (an object with a discrete translation symmetry). To represent a code, it is useful to arrange the vectors $\vec{s}_i$ in a $2n \times 2n$ matrix

$$S = \begin{pmatrix} \vec{s}_1^\top \\ \vec{s}_2^\top \\ \vec{s}_3^\top \\ \dots \end{pmatrix}.$$

The grid points of the lattice Λ can then be expressed as the set

$$\Lambda = \{S^\top \vec{a} : \vec{a} \in \mathbb{Z}^{2n}\},$$

where the vector $\vec{a} \in \mathbb{Z}^{2n}$ essentially labels the grid points $(00, 10, 01, 11, \dots)$.

What remains to understand is how we can perform operations on the codewords, i.e. what are Pauli operators? For that, notice that a code is valid (i.e. its stabilizers all commute with each other) if

$$S\Omega S^\top = A \in \mathbb{Z}^{2n \times 2n}, \tag{19}$$

that is if the matrix A encoding the commutation relations contains only integers: this equation is a generalization of equation 17. We can generalize this further to look for all valid operations on the code, which must commute with the stabilizers, $[\hat{D}(\vec{v}), \hat{D}(\vec{s}_j)] = 0$. This amounts to finding the set of vectors $\vec{v}$ that satisfy

$$S\Omega\vec{v} \in \mathbb{Z}^{2n}$$

such that we can construct the group of all valid operations[9]

$$\Lambda^* = \{\vec{v} : S\Omega\vec{v} \in \mathbb{Z}^{2n}\},$$

given by the lattice dual to Λ (see box about dual lattice). Note that the set Λ^* contains Λ, as can be seen from equation 19, but not only. It additionally gives us the set of Pauli operations: These are operations that commute with the stabilizers (and hence are "transparent") to them, but still can modify the codewords.

[9] for QEC aficionados, this is the normalizer of the stabilizer group. Also notice that we identify operators by their vectors. The vectors don't form a group, but the translation operators associated to them do.

Dual Lattice

Consider a lattice[a] Λ. The Euclidian dual of a lattice Λ is

$$\Lambda^{\perp} = \{\vec{p} : \vec{p} \cdot \vec{s} \in \mathbb{Z} \quad \forall \vec{s} \in \Lambda\}$$

This is analogous to real vs reciprocal lattice in solid state physics. A large real space lattice will give rise to a small reciprocal lattice, and vice versa. However, in phase space the geometry is not Euclidian, i.e. we can't use the dot product $\vec{u} \cdot \vec{v}$ but rather we need to use the symplectic form $\vec{u}^{\top}\Omega\vec{v}$. This measures the oriented area between vectors, rather than their relative projection like the dot product. Using this metric, we can define the symplectic dual lattice

$$\Lambda^* = \{\vec{v} : \vec{s}^{\top}\Omega\vec{v} \in \mathbb{Z} \quad \forall \vec{s} \in \Lambda\} = \{\vec{v} : S\Omega\vec{v} \in \mathbb{Z}^{2n}\}.$$

Constructing the dual lattice is straightforward. First, define

$$A = S\Omega S^{\top}.$$

The matrix A is called the symplectic Gram matrix. Note that $A^{\top} = -A$. If it is invertible (which for our codes it is), it can be used to generate a matrix S^* that defines the dual lattice

$$S^* = A^{-1}S$$

in the sense that

$$\Lambda^* = \{(S^*)^{\top}\vec{a} : \vec{a} \in \mathbb{Z}^{2n}\}.$$

Elements of Λ^* generated in this manner are part of the dual lattice. To show that, we need to check that $\vec{\lambda}^* = (S^*)^{\top}\vec{a}$ is part of the dual lattice:

$$S\Omega\vec{\lambda}^* \overset{?}{\in} \mathbb{Z}^{2n} \text{(Condition for being in dual lattice)}$$
$$S\Omega(S^*)^{\top}\vec{a} = S\Omega S^{\top}A^{-\top}\vec{a} = AA^{-\top}\vec{a} = A(-A^{-1})\vec{a} = -\vec{a} \in \mathbb{Z}^{2n}$$

So S^* generates lattice points in Λ^*. Since there are $2n$ vectors in S^* we have found a set of vectors that completely describes the dual lattice (this is not a rigorous proof).

[a] Here Λ is a set of points $\{\vec{v}_1, \vec{v}_2, ...\}$ forming a lattice. It has a matrix S associated that defines a unit cell.

10.3 Pauli operators

Now, what are the Pauli operators? To understand how to construct them, it is useful to take the example of the $d = 2$ square code, see how operators appear

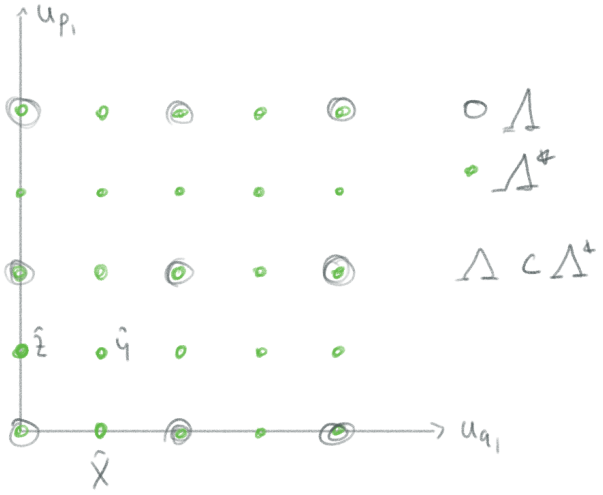

there, and generalize this. This code is generated by the matrix

$$S_2 = \begin{pmatrix} \sqrt{2} & 0 \\ 0 & \sqrt{2} \end{pmatrix}.$$

We can verify it's a valid code because

$$S_2 \Omega S_2^\top = 2\Omega = \begin{pmatrix} 0 & 2 \\ -2 & 0 \end{pmatrix} = A \in \mathbb{Z}^{2\times 2}$$

where A the symplectic Gram matrix. From there, we can generate the dual lattice

$$S^* = A^{-1}S = \begin{pmatrix} 0 & -\frac{1}{2} \\ \frac{1}{2} & 0 \end{pmatrix} \begin{pmatrix} \sqrt{2} & 0 \\ 0 & \sqrt{2} \end{pmatrix} = \begin{pmatrix} 0 & -\frac{\sqrt{2}}{2} \\ \frac{\sqrt{2}}{2} & 0 \end{pmatrix}.$$

We can represent the lattice and its dual in phase space:

The stabilizers form the larger grid, and we find three operators $(\hat{X}, \hat{Y}, \hat{Z})$ that are valid operations but not stabilizers. These then form the Pauli group. Notice that any displacement operator has to fit inside Λ's unit cell (because translating by any stabilizer vector acts as the identity on codewords, any displacement operator is equivalent to one within Λ's unit cell), such that we can geometrically find the order (=number of elements) of the group of non-trivial operators, which we will identify with the Pauli group. The way to do this is to check the volume of the unit cell, and see how many dual lattice unit cells fit in:

$$\frac{\det S}{\det S^*} = \frac{\det S}{\det A^{-1} \det S} = \frac{1}{\det A^{-1}} = \det A$$

Up to the phases, the qudit Pauli group has d^2 elements, such that to construct a qudit code we need to fit d^2 operators from Λ^* into Λ, hence a further condition for a valid qudit code is that

$$\det A = d^2.$$

10.4 Code Gauges

One has to be careful about a subtelty now. Naïvely, one might think that every point in the lattice can be associated to a stabilizer operator. In other words, if $\hat{D}(\vec{s}_1), \hat{D}(\vec{s}_2)$ are stabilizers, then one might think that $\hat{D}(\vec{s}_1 + \vec{s}_2)$ also must be a stabilizer. This is not quite true: For $\vec{s}_1^\top \Omega \vec{s}_2 = 2\pi$, we have $\hat{D}(\vec{s}_1 + \vec{s}_2) |\psi\rangle = e^{\frac{il^2}{2} \vec{s}_1^\top \Omega \vec{s}_2} \hat{D}(\vec{s}_1)\hat{D}(\vec{s}_2) |\psi\rangle = e^{i\pi} |\psi\rangle = -|\psi\rangle$. In this way, we can distinguish a positive and a negative lattice, where

$$\Lambda_\nu = \{\vec{s} : \hat{D}(\vec{s}) |\psi\rangle = \nu |\psi\rangle \quad \forall |\psi\rangle \in \mathcal{C}\}$$

with $\nu = +1$ or $\nu = -1$. So a given lattice offers several choices of stabilizers. Given such a choice, encapsulated as a matrix S and its associated stabilizers $\vec{s}_j$, we can define a *gauge* $\vec{\mu} \in \mathbb{Z}_2^{2n}$

$$\hat{D}(\vec{s}_j) |\psi\rangle = (-1)^{\mu_j} |\psi\rangle .$$

From a single lattice we can therefore construct different sets of stabilizer operators labeled by their gauge $\vec{\mu}$. But how does changing gauge affect the codewords? Assume we want to change the gauge of a codeword $|\psi\rangle_0$ to $|\psi\rangle_1$ by using a translation $\hat{D}(\vec{v})$:

$$-|\psi\rangle_1 = \hat{D}(\vec{s}_1) |\psi\rangle_1 = \hat{D}(\vec{s}_1)\hat{D}(\vec{v}) |\psi\rangle_0 = e^{il^2 \vec{s}_j^\top \Omega \vec{v}} \hat{D}(\vec{v}) |\psi\rangle_0 \to \vec{s}_j^\top \Omega \vec{v} = 1/2,$$

which means that to change a gauge, one needs to translate the codword by half a dual lattice vector. Different gauges will have different codewords, but they will all have the same lattice symmetry (grid spacing, etc.). They will simply be half-dual translations of each other. As we'll see later, in the single-mode qubit case, there is only a positive lattice, but we will encounter situations where switching the gauge or combining different gauges for multiple modes can be useful, hence we introduced it here.

Let's go through a few examples to build a bit of intuition.

10.5 Examples of GKP codes

The qunaught code Let's start with the simplest code, $d = 1$. We call this the qunaught code because it encodes *naught* information. The generating

matrix is

$$S = \begin{pmatrix} 1 & 0 \\ 0 & 1 \end{pmatrix} = \mathbb{1}$$

the Gram matrix is

$$A = S\Omega S^\top = \Omega = \begin{pmatrix} 0 & 1 \\ -1 & 0 \end{pmatrix} \in \mathbb{Z}^{2\times 2}$$

and the dual lattice generator is

$$S^* = A^{-1}S = \Omega^{-1} = \Omega^\top = \begin{pmatrix} 0 & -1 \\ 1 & 0 \end{pmatrix}$$

such that the dual lattice is the lattice itself. Computing the determinant of A gives us the dimension of the qudit code

$$\det A = 1 = d^2 \Rightarrow d = 1$$

this means that we have a $U(1)$ symmetry in the code. Or in other words, there are no elements of the dual lattice that are not also in the real (stabilizer) lattice. Hence, we cannot perform any logical operations on a qunaught, it's not a qubit code, the logical subspace of the code has dimension 1. However, the qunaught code is a useful resource in many protocols, so we still want to study it further. The next question to ask is that of the codewords. From S we can construct a stabilizer group (up to a gauge choice)

$$\mathcal{S}_{(0,0)} = \left\{ \hat{D}\begin{pmatrix} 1 \\ 0 \end{pmatrix}, \hat{D}\begin{pmatrix} 0 \\ 1 \end{pmatrix} \right\}.$$

The codewords

$$|\emptyset\rangle = \sum_{k=-\infty}^{\infty} |q = \sqrt{2\pi}k\rangle$$

are eigenstates of these operators, indeed

$$\hat{D}\begin{pmatrix} 1 \\ 0 \end{pmatrix} |\emptyset\rangle = e^{il\hat{p}} |\emptyset\rangle = \sum_{k=-\infty}^{\infty} |q = \sqrt{2\pi}k + l\rangle = |\emptyset\rangle$$

with $l = \sqrt{2\pi}$, and

$$\hat{D}\begin{pmatrix} 0 \\ 1 \end{pmatrix} |\emptyset\rangle = e^{-il\hat{q}} \sum_{k=-\infty}^{\infty} |q = \sqrt{2\pi}k\rangle = e^{-i2\pi k} \sum_{k=-\infty}^{\infty} |q = \sqrt{2\pi}k\rangle = |\emptyset\rangle .$$

The set $\mathcal{S}$ that we chose is not unique. We could have chosen instead

$$\mathcal{S}_{(0,1)} = \left\{ \hat{D}\begin{pmatrix} 1 \\ 0 \end{pmatrix}, \hat{D}\begin{pmatrix} 1 \\ 1 \end{pmatrix} \right\}.$$

Do we still have the same codewords? We know that $\hat{D}(1,0)^\top$ is a stabilizer, however notice that

$$\hat{D}\begin{pmatrix}1\\1\end{pmatrix}|\emptyset\rangle = -\hat{D}\begin{pmatrix}1\\0\end{pmatrix}\hat{D}\begin{pmatrix}0\\1\end{pmatrix}|\emptyset\rangle = -|\emptyset\rangle$$

Such that the updated set of stabilizers requires different codewords. If we translate the original codeword $|\emptyset\rangle$ by half a lattice, we again obtain a codeword, but in a different gauge (which we now label $(0,1)$. Defining

$$|\emptyset\rangle_{(0,1)} = \sum_{k=-\infty}^{\infty} |q = \sqrt{2\pi}(k+1/2)\rangle$$

we obtain again a codeword since

$$\hat{D}\begin{pmatrix}1\\0\end{pmatrix}|\emptyset\rangle_{(0,1)} = e^{il\hat{p}}|\emptyset\rangle_{(0,1)} = \sum_{k=-\infty}^{\infty} |q = \sqrt{2\pi}(k+1/2)+l\rangle = |\emptyset\rangle_{(0,1)}$$

and

$$\begin{aligned}
\hat{D}\begin{pmatrix}1\\1\end{pmatrix}|\emptyset\rangle_{(0,1)} &= -\hat{D}\begin{pmatrix}1\\0\end{pmatrix}\hat{D}\begin{pmatrix}0\\1\end{pmatrix}|\emptyset\rangle_{(0,1)} \\
&= -\hat{D}\begin{pmatrix}1\\0\end{pmatrix} e^{-il\hat{q}} \sum_{k=-\infty}^{\infty} |q = \sqrt{2\pi}(k+1/2)\rangle \\
&= -\hat{D}\begin{pmatrix}1\\0\end{pmatrix} e^{-i2\pi k - i\pi} \sum_{k=-\infty}^{\infty} |q = \sqrt{2\pi}(k+1/2)\rangle \\
&= \hat{D}\begin{pmatrix}1\\0\end{pmatrix}|\emptyset\rangle_{(0,1)} \\
&= |\emptyset\rangle_{(0,1)}
\end{aligned}$$

This is the same code, but in a different gauge! The qunaught code admits four different gauges, $(0,0),(0,1),(1,0),(1,1)$ and they correspond to lattices that are shifted by half a lattice constant.

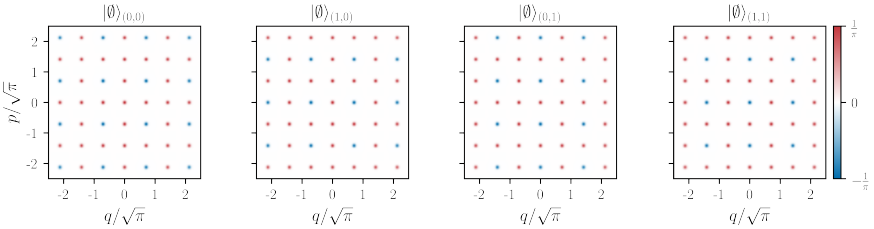

Wigner functions of the four qunaught gauge states

The qunaught code can be understood as the smallest and most primitive example of a grid state, and is used found in many state preparation and teleportation protocols. But it doesn't encode any information yet!

The square qubit code We already encountered the S matrix of the square qubit code when I introduced the dual lattice, recall that we have

$$S_2 = \begin{pmatrix} \sqrt{2} & 0 \\ 0 & \sqrt{2} \end{pmatrix}.$$

we also generated the dual lattice already

$$S^* = A^{-1}S = \begin{pmatrix} 0 & -\frac{\sqrt{2}}{2} \\ \frac{\sqrt{2}}{2} & 0 \end{pmatrix}.$$

and found the associated logical Pauli operators

$$\hat{X} = \hat{D}\begin{pmatrix} \frac{1}{\sqrt{2}} \\ 0 \end{pmatrix}, \hat{Z} = \hat{D}\begin{pmatrix} 0 \\ \frac{1}{\sqrt{2}} \end{pmatrix} \Rightarrow \hat{Y} = \frac{\hat{X}\hat{Z}}{i} = \hat{D}\begin{pmatrix} \frac{1}{\sqrt{2}} \\ \frac{1}{\sqrt{2}} \end{pmatrix}$$

The stabilizers are given by

$$\mathcal{S} = \left\{ \hat{D}\begin{pmatrix} \sqrt{2} \\ 0 \end{pmatrix}, \hat{D} = \begin{pmatrix} 0 \\ \sqrt{2} \end{pmatrix} \right\} = \left\{ \hat{S}_X, \hat{S}_Z \right\}$$

and the codewords by

$$\mathcal{C} = \{|0\rangle, |1\rangle\}, |0\rangle = \sum_{k=-\infty}^{\infty} |q = 2\sqrt{\pi}k\rangle, |1\rangle = \sum_{k=-\infty}^{\infty} |q = 2\sqrt{\pi}(k + \tfrac{1}{2})\rangle.$$

We verify their properties. First, are they indeed stabilizer eigenstates? Yes:

$$\begin{aligned} \hat{D}\begin{pmatrix} \sqrt{2} \\ 0 \end{pmatrix}|0\rangle &= e^{i2\sqrt{\pi}\hat{p}}|0\rangle \\ &= \sum_{k=-\infty}^{\infty} |q = 2\sqrt{\pi}k + 2\sqrt{\pi}\rangle \\ &= |0\rangle \\ \hat{D}\begin{pmatrix} 0 \\ \sqrt{2} \end{pmatrix}|0\rangle &= e^{-i2\sqrt{\pi}\hat{q}}|0\rangle \\ &= \sum_{k=-\infty}^{\infty} e^{-4i\pi k}|q = 2\sqrt{\pi}k\rangle \\ &= |0\rangle, \end{aligned}$$

and the derivation is similar for $|1\rangle$. We look at the action of the logical Paulis

on the state $|1\rangle$

$$\begin{aligned}
\hat{X}|1\rangle = \hat{D}\begin{pmatrix}\frac{\sqrt{2}}{2}\\ 0\end{pmatrix}|1\rangle &= e^{i\sqrt{\pi}\hat{p}}|1\rangle \\
&= \sum_{k=-\infty}^{\infty} |q = 2\sqrt{\pi}(k+\tfrac{1}{2}) + \sqrt{\pi}\rangle \\
&= \sum_{k=-\infty}^{\infty} |q = 2\sqrt{\pi}k\rangle \\
&= |0\rangle \\
\hat{Z}|1\rangle = \hat{D}\begin{pmatrix}0\\ \frac{\sqrt{2}}{2}\end{pmatrix}|1\rangle &= e^{-i\sqrt{\pi}\hat{q}}|1\rangle \\
&= \sum_{k=-\infty}^{\infty} e^{-2i\pi(k+\frac{1}{2})}|q = 2\sqrt{\pi}(k+\tfrac{1}{2})\rangle \\
&= -|1\rangle\,,
\end{aligned}$$

Finally, notice that we have that $\hat{X}^2 = \hat{S}_x$ and $\hat{Z}^2 = \hat{S}_Z$ which are identities on the codespace.

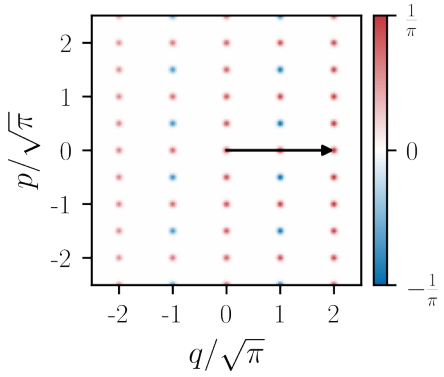

The arrow shows $\hat{S}_x$

Often times, codes will have links to each other, as lattices can be cast into each other. In the case of the square qubit code, the square GKP Y eigenstate is in fact a rotated $|\emptyset\rangle_{(0,1)}$ state, which is useful because the latter can be easier to prepare. Interestingly, the square qubit code only admits one gauge ($\vec{\mu} = (0,0)$), as its stabilizers enclose an area of 4π.

The diamond code A $\pi/4$ rotation of the square GKP code gives the diamond code:

$$S = \begin{pmatrix}1 & 1\\ 1 & -1\end{pmatrix}$$

It is equivalent to the square GKP code, but sometimes used in code switching procedures, hence we mention it here.

Pauli qudit operators

For a qubit ($d = 2$), the Pauli group is essentially described by $\hat{X}_2, \hat{Z}_2$ through the relations

$$\hat{X}_2\hat{Z}_2 = -\hat{Z}_2\hat{X}_2, \hat{X}_2^2 = \hat{Z}_2^2 = \mathbb{1}$$

The elements of the $d = 2$ Pauli group is the set of 16 elements

$$\mathcal{P}_2 = \{i^k \hat{X}_2^a \hat{Z}_2^b : k, a, b \in \mathbb{Z}\} = \{\mathbb{1}, \hat{X}, \hat{Y}, \hat{Z}, i\mathbb{1}, i\hat{X}, \dots\}$$

This generalizes to d. Define $\omega = \exp(2\pi i/d)$, the Pauli algebra relations become

$$\hat{X}_d\hat{Z}_d = \omega^{-1}\hat{Z}_d\hat{X}_d, \quad \hat{X}_d^d = \hat{Z}_d^d = \mathbb{1}$$

$\hat{X}_d$ is called the shift and $\hat{Z}_d$ the clock operator. The d-dimensional Pauli group is the set of elements

$$\mathcal{P}_d = \{\omega^k \hat{X}_d^a \hat{Z}_d^b : k, a, b \in \mathbb{Z}\}$$

A little quirk is the order of the group, that is the number of elements of the set. In odd d, there are d^3 elements, whereas in even d, there are $2d^3$ elements. The states are now labeled

$$|0\rangle, |1\rangle, \dots |d-1\rangle$$

and the operators act as

$$\hat{X}_d |j\rangle = |j + 1 \bmod d\rangle, \quad \hat{Z}_d |j\rangle = \omega^j |j\rangle.$$

Typically we omit the subscripts $\hat{X}_d \to \hat{X}$ and infer the dimension from context.

The single-mode square qudit code One does not need to stop at a qubit for encoding information. We can in fact encode any qudit of dimension d into an oscillator, by using the code defined by the stabilizers

$$S = \begin{pmatrix} \sqrt{d} & 0 \\ 0 & \sqrt{d} \end{pmatrix}$$

we verify it's a valid code by checking

$$S\Omega S^\top = d\Omega = A \in \mathbb{Z}^{2\times 2}$$

and the code dimension is

$$\det A = d^2.$$

The dual lattice is generated by

$$S^* = \frac{1}{\sqrt{d}} \begin{pmatrix} 0 & -1 \\ 1 & 0 \end{pmatrix}$$

and the logical qudit Pauli operators (see box about Pauli qudit operators) are then given by

$$\hat{X}_d = \hat{D} \begin{pmatrix} \frac{1}{\sqrt{d}} \\ 0 \end{pmatrix}, \hat{Z}_d = \hat{D} \begin{pmatrix} 0 \\ \frac{1}{\sqrt{d}} \end{pmatrix}.$$

The codewords are

$$\begin{aligned} |0\rangle &= \sum_{k=-\infty}^{\infty} |q = \sqrt{2\pi d} k\rangle \\ |1\rangle &= \sum_{k=-\infty}^{\infty} |q = \sqrt{2\pi d}\,(k + \tfrac{1}{d})\rangle \\ |j\rangle &= \sum_{k=-\infty}^{\infty} |q = \sqrt{2\pi d}\left(k + \frac{j}{d}\right)\rangle \\ |d-1\rangle &= \sum_{k=-\infty}^{\infty} |q = \sqrt{2\pi d}\,(k + \tfrac{d-1}{d})\rangle \end{aligned}$$

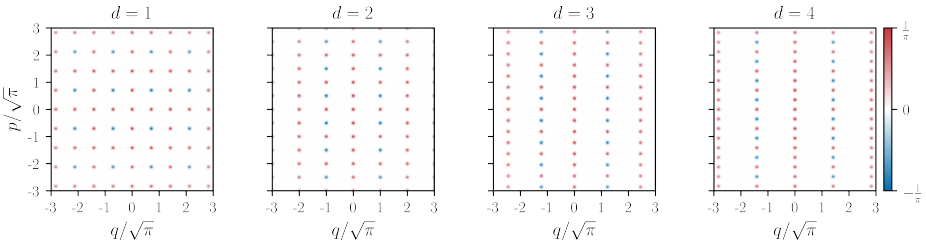

Wigner functions of $|0\rangle$ states of a qudit

The tesseract code Finally, we now consider a non-trivial 2-mode code: the tesseract code, with its S matrix given by

$$S = \sqrt[4]{2} \begin{pmatrix} 1 & 0 & 0 & 0 \\ 0 & 1/\sqrt{2} & 0 & 1/\sqrt{2} \\ 0 & 0 & 1 & 0 \\ 0 & 1/\sqrt{2} & 0 & -1/\sqrt{2} \end{pmatrix}$$

The lattice in question is a square lattice in which the $p_1 - p_2$ plane got rotated by 45°, which gives it interesting QEC properties as we'll see later.

We check that it's a valid code by calculating its symplectic Gram matrix

$$S\Omega S^\top = \sqrt[4]{2}\begin{pmatrix}1 & 0 & 0 & 0\\ 0 & \frac{1}{\sqrt{2}} & 0 & \frac{1}{\sqrt{2}}\\ 0 & 0 & 1 & 0\\ 0 & \frac{1}{\sqrt{2}} & 0 & -\frac{1}{\sqrt{2}}\end{pmatrix}\begin{pmatrix}0 & 1 & 0 & 0\\ -1 & 0 & 0 & 0\\ 0 & 0 & 0 & 1\\ 0 & 0 & -1 & 0\end{pmatrix}\sqrt[4]{2}\begin{pmatrix}1 & 0 & 0 & 0\\ 0 & \frac{1}{\sqrt{2}} & 0 & \frac{1}{\sqrt{2}}\\ 0 & 0 & 1 & 0\\ 0 & \frac{1}{\sqrt{2}} & 0 & -\frac{1}{\sqrt{2}}\end{pmatrix}^\top$$
$$= \begin{pmatrix}0 & 1 & 0 & 1\\ -1 & 0 & -1 & 0\\ 0 & 1 & 0 & -1\\ -1 & 0 & 1 & 0\end{pmatrix} = A \in \mathbb{Z}^{4\times 4}$$

The determinant gives us the code dimension

$$\det A = 4 = d^2,$$

so it's a qubit code. We can calculate its dual lattice generator

$$S^* = A^{-1}S = \begin{pmatrix}0 & -1 & 0 & 0\\ \frac{1}{\sqrt{2}} & 0 & \frac{1}{\sqrt{2}} & 0\\ 0 & 0 & 0 & -1\\ \frac{1}{\sqrt{2}} & 0 & -\frac{1}{\sqrt{2}} & 0\end{pmatrix}$$

In the qubit case, we had two columns such that it was easy to choose two operators that we associate to X and Z. Here, the situation is more complex and we have to make a choice of Pauli operators. A possible choice is

$$\hat{X} = \hat{D}\left(\sqrt[4]{2}\begin{pmatrix}\frac{1}{2}\\ 0\\ \frac{1}{2}\\ 0\end{pmatrix}\right), \hat{Y} = \hat{D}\left(\sqrt[4]{2}\begin{pmatrix}\frac{1}{2}\\ \frac{1}{\sqrt{2}}\\ \frac{1}{\sqrt{2}}\\ 0\end{pmatrix}\right), \hat{Z} = \begin{pmatrix}0\\ \frac{1}{\sqrt{2}}\\ 0\\ 0\end{pmatrix}.$$

Many other higher-dimensional multi-mode qubit codes exist, and if they interest you I highly recommend reading Baptiste Royer's paper exploring the various codes.

11 Bringing codes into reality

11.1 Errors in trapped ion oscillators

When looking at quantum error correction codes, we of course have to consider which errors are likely to happen in our system. It turns out that in trapped ions, a good error model is that of a very weakly coupled hot (300K) bath. In a way, this reflects the experimental setup, where an ion is trapped and very well isolated, but its surroundings can be at room temperature or in more recent setups also cryogenic (typically 4K), surroundings to which the ion couples weakly and with which it can exchange energy.

To give a bit of a feeling for orders of magnitude, a 2 MHz oscillator (our ion) held at room temperature has a mean phonon number $\bar{n}_{th} \approx 3 \cdot 10^6$. Using various methods of laser cooling, one can go to the ground state $n = 0$. In good setups, we observe a heating rate (i.e. how long it takes to acquire one quantum after ground state cooling) of $\dot{\bar{n}} \approx 0.1 - 10$ q/s (quanta per second). This heating can be modelled by representing the bath $\hat{b}$ as a thermal state with $\bar{n}_{th}$ to which the ion is weakly coupled $\hbar\kappa(\hat{a}\hat{b}^\dagger + \hat{b}\hat{a}^\dagger)$. Tracing out the bath (for details see more specialized textbooks/lectures) we arrive at collapse operators modelling the system that have the form

$$\hat{c}_+ = \sqrt{\kappa_+}\hat{a}^\dagger, \quad \hat{c}_- = \sqrt{\kappa_-}\hat{a}$$

where $\kappa_+ = \kappa(\bar{n}_{th})$ and $\kappa_- = \kappa(\bar{n}_{th} + 1)$. To see how this causes heating, let's compare the probabilities P_+ and P_- of a heating ($\hat{c}_+$) and a loss ($\hat{c}_-$) event during a time $dt \ll \kappa_\pm^{-1}$ and for $n \ll \bar{n}_{th}$.

$$P_+ = \kappa_+ \langle n| \hat{a}\hat{a}^\dagger |n\rangle \, dt = \kappa_+(n+1)dt$$

and

$$P_- = \kappa_- \langle n| \hat{a}^\dagger\hat{a} |n\rangle \, dt = \kappa_- n dt$$

The heating rate is given[10] by $(P_+ - P_-)/dt$ and therefore we have that

$$\dot{\bar{n}} = \frac{P_+ - P_-}{dt} = \frac{\kappa_+(n+1)dt - \kappa_- n dt}{dt} = \frac{\kappa_+ dt + n(\kappa_+ - \kappa_-)dt}{dt} \approx \kappa\bar{n}_{th}$$

Plugging in the numbers from earlier, we find that $\kappa \approx 10^{-6}$ (weak coupling) for $n_{th} \approx 10^6$. Counterintuively, this means that $\kappa_+ \approx \kappa_- = \bar{\kappa}$ and we could model this process using the error channel

$$\mathcal{E} = \left\{ \mathbb{1} - \frac{\bar{\kappa}dt}{2}(2\hat{a}^\dagger\hat{a} + 1), \sqrt{\bar{\kappa}dt}\hat{a}^\dagger, \sqrt{\bar{\kappa}dt}\hat{a} \right\}$$

[10] Try to prove it!

Now, since GKP states are good against displacements, we will play a trick. Collapse operator sets which are linear combinations of each other are equivalent, which allows us to write can write $\hat{a}, \hat{a}^\dagger$ as approximations of displacement operators, using $\epsilon = \sqrt{\bar{\kappa} dt} \ll 1$:

$$\epsilon\hat{a} = \frac{\epsilon}{\sqrt{2}}(\hat{q} + i\hat{p}) \approx \frac{1}{\sqrt{2}}(\sin(\epsilon\hat{q}) + i\sin(\epsilon\hat{p})) = \frac{1}{2\sqrt{2}i}(e^{i\epsilon\hat{q}} - e^{-i\epsilon\hat{q}} + ie^{i\epsilon\hat{p}} - ie^{-i\epsilon\hat{p}})$$

$$\epsilon\hat{a}^\dagger = \frac{\epsilon}{\sqrt{2}}(\hat{q} - i\hat{p}) \approx \frac{1}{\sqrt{2}}(\sin(\epsilon\hat{q}) - i\sin(\epsilon\hat{p})) = \frac{1}{2\sqrt{2}i}(e^{i\epsilon\hat{q}} - e^{-i\epsilon\hat{q}} - e^{i\epsilon\hat{p}} + e^{-i\epsilon\hat{p}})$$

From here it's clear that the error set should contain displacement operators, and it turns out that the correct error channel (which conserves trace) for small enough timescales ($\bar{\kappa} dt \ll 1$) can be written as

$$\mathcal{E} = \left\{\mathbb{1}(1 - 4\bar{\kappa} dt), \sqrt{\bar{\kappa} dt} e^{i\sqrt{\bar{\kappa} dt}\hat{p}}, \sqrt{\bar{\kappa} dt} e^{-i\sqrt{\bar{\kappa} dt}\hat{p}}, \sqrt{\bar{\kappa} dt} e^{i\sqrt{\bar{\kappa} dt}\hat{q}}, \sqrt{\bar{\kappa} dt} e^{-i\sqrt{\bar{\kappa} dt}\hat{q}}\right\}.$$

There are two interesting observations here: first, in this description, we no longer have the $\hat{a}^\dagger a$ term. Secondly, and more importantly, given that we correct quickly enough, errors on the oscillator may be decomposed (at least approximately) as displacements! And as we already have seen, the GKP code is robust against them.

This means that displacement errors are approximately equivalent to phonon gain and loss errors. It turns out that GKP codes are optimal against displacement (gain/loss) errors[11], such that if the dominant noise is heating/cooling then it is a good code for the platform.

The other leading type of error in a typical oscillators is dephasing. Dephasing can be understood as random fluctuations of the oscillator's frequency, leading to the error set given a dephasing rate γ_ϕ

$$\mathcal{E} = \left\{1 - \frac{\gamma_\phi dt}{2}\hat{n}^2, \sqrt{\gamma_\phi dt}\hat{n}\right\}.$$

GKP codes are not well suited against dephasing, for which cat states perform much better. GKP codes are able to correct for limited amounts of dephasing, though, and the intuition behind which errors can be corrected or not will be explored in the next section.

11.1.1 Voronoi cell and correctable errors

We have seen that we can decompose errors in oscillators as small displacements. But which errors are correcteable? To answer that, we need to understand how an optimal decoder would work. We can rephrase the question we just asked for

[11] Albert, V.V., et al., *Performance and structure of single-mode bosonic codes*, Physical Review A, v. 97, no. 3, p. 032346.

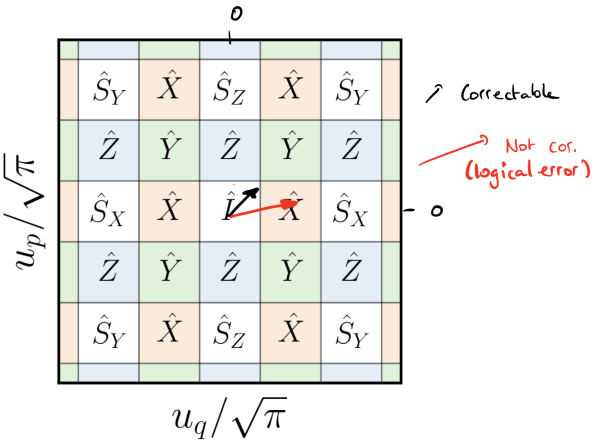

Figure 31: GKP tile. The center of each square is associated to a dual lattice point, and the region around it is its Voronoi cell. An optimal decoder would simply measure a displacement and push it back to the closest point with a cell.

displacement errors: Assume we have a displacement error of length ϵ. What is the biggest tolerable ϵ? To answer that, consider again the GKP state. Recall that to each point in the GKP grid (dual lattice), we can associate an operation (see figure 31). Notice that the grid will get displaced by the error, but as long as the displacement is smaller than half a dual lattice spacing (i.e. it stays in a cell), we can uniquely identify which point came from where. This region of correctable points is called a Voronoi cell of a code. If the displacement leaves the Voronoi cell, then we have a logical error (red arrow below) associated to the closest operator in the dual lattice (e.g. $\hat{X}$ error in the example below). This also shows how robustness to single-qubit gates can be obtained, as a gate can be imperfect given a subsequent perfect error correction cycle.

11.2 Finite energy effects and realistic states

The states we have considered so far are not physical states. Consider for example the GKP 0 eigenstate

$$|0\rangle = \sum_{k=-\infty}^{\infty} |k = 2\sqrt{\pi}k\rangle \,.$$

Both the position eigenstate and the fact that we take an infinite sum over them are non-physical. To bring the states into reality, one applies an envelope operator $\hat{\mathcal{E}}$

$$\hat{\mathcal{E}}_\Delta = \exp(-\Delta^2 \hat{n}), \quad \hat{n} = \bigotimes_{j=0}^{n-1} \hat{n}_j$$

where $\hat{n}_j = \hat{a}_j^\dagger \hat{a}_j$. The infinite-energy GKP state's wavefunction is a superposition of delta peaks, and this operator effectively both reduces the spatial extent (suppressing peaks far away from the origin) at the expense of broadening them. Note that the operator is not unitary, hence the states need to be normalized after the application.

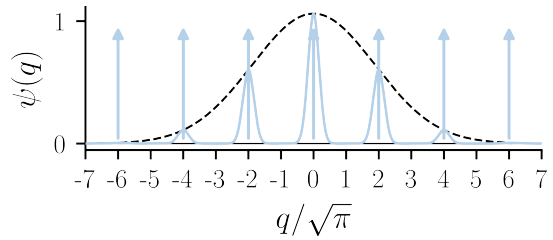

Figure 32: Finite-energy GKP state (Gaussian comb) versus ideal state (delta functions)

In particular, after application of the envelope operator the $|0\rangle$ GKP state becomes

$$|0\rangle_L \propto \sum_{n\in\mathbb{N}} \exp(-\tfrac{1}{2}\Delta^2(2n\sqrt{\pi})^2)\hat{D}\begin{pmatrix}2n\sqrt{\pi}\\0\end{pmatrix}|\Delta\rangle_q$$

where $|\Delta\rangle_q$ is a Gaussian state

$$\langle q|\Delta\rangle = \left(\frac{1}{\pi\Delta^2}\right)^{\frac{1}{4}} \exp\left(\frac{-q^2}{2\Delta^2}\right).$$

Note that in the limit $\Delta \to 0$ one recovers the ideal codewords, as the gaussian converges to a delta function and the spatial extent of the wavefunction increases. The envelope parameter Δ is often referred to as squeezing parameter, as the Gaussian wavepackets can be understood as squeezed displaced vacuum states. In the literature, the quality of GKP states is therefore often described in terms of its effective squeezing parameter

$$\Delta_{\text{dB}} = -20\log_{10}(\Delta)$$

expressed in decibels.

How good does a GKP state need to be in order to perform some useful (fault-tolerant) computation with it? Studies[12] have shown that roughly 10 dB are sufficient, if properly combined with other techniques. One of these techniques is a first layer of QEC.

[12]Bourassa, J.E., et al, *Blueprint for a Scalable Photonic Fault-Tolerant Quantum Computer*: Quantum, v. 5, p. 392.

11.3 Operations on Finite-energy states

So far, so good. But how does one prepare and control these states?

11.3.1 State preparation

Preparing a GKP state is a non-trivial task. There are theorems that show that it's impossible to prepare a GKP state using displacements and squeezing alone (Gaussian operations), one needs an inherently non-linear resource (either homodyne measurement or qubit-controlled operations). The non-linear resource used in superconducting cavities and trapped ions is the state-dependent force (conditional displacement). Recall that the Hamiltonian it implements has the form

$$e^{-i\alpha\hat{q}\hat{\sigma}_x}$$

such that it can both displace conditioned on the spin, but also perform a spin-rotation conditioned on position. In trapped ions, the way a GKP states is prepared state is shown on figure 33 We start by preparing a $|n=0\rangle$ motional ground state. We then position-squeeze it in order to prepare the central peak of the GKP state. We then need a non-linearity, in the case of a trapped ion the internal degree of freedom (spin). State-dependent force are applied to displace and disentangle in a way that builds up the GKP comb.

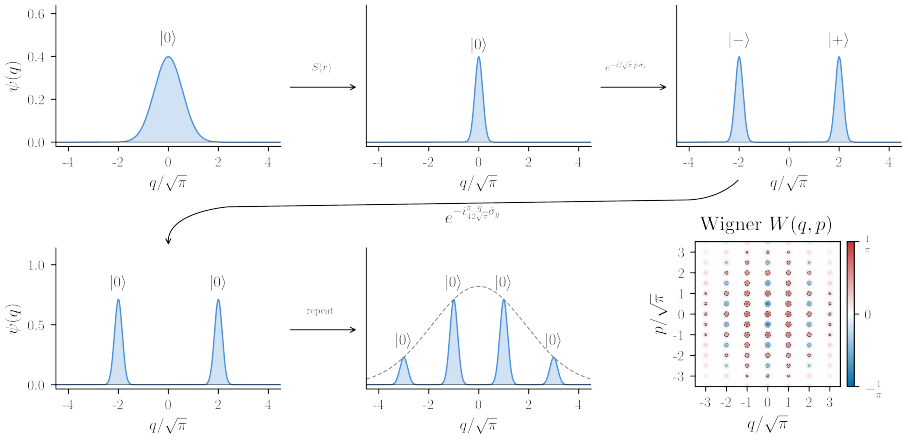

Figure 33: State preparation of a GKP state. For further reading, see *Measurement-Free Preparation of Grid States*, Hastrup et al.

There exist other methods to prepare GKP state, including ones which involve optimal control pulse sequences (see e.g. V. Matsos et al.).

11.3.2 Readout

The next challenge is reading out the GKP state. One possibility is doing homodyne detection, which directly allows measuring $\hat{q}$. For example to read out in the Z basis, one would measure the quadrature $\hat{q}$. The outcome of this measurement is a number, for example $1.002\sqrt{\pi}$. One would then infer that we had a $|1\rangle$ GKP state. This is very hard, however, in practice, and furthermore homodyne detection is not possible and in a trapped ion setting at the resolution necessary.

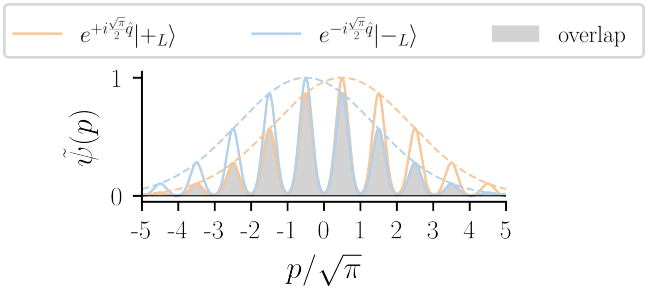

Figure 34

Therefore, we resort once again to the state-dependent force. Naively, one might think that it is possible to simply measure directly a logical operator (e.g. $\hat{Z} = e^{-i\sqrt{\pi}\hat{q}}$) on a $|0\rangle$ eigenstate. One could think to do this via a state-dependent force again using, $e^{-i\sqrt{\pi}/2\sigma_x}$ and reading out the spin afterwards. This is however - as is shown in the exercises, not quite possible as one loses contrast due to a loss in overlap when using a finite-energy state (see figure 34). As is shown in the exercises, this overlap loss is substantial, and it scales as $e^{-\pi/4\Delta^2}$.

To overcome this problem, once again we can play a trick involving a state-dependent force. Restating the problem we previously had, the state-dependent force broadens the state along the axis opposite to which we want to measure. This is because it always can be interpreted both as a spin-rotation that depends on position (the bit we want to readout the state) and as an actual force (along the momentum axis). To counteract that, the idea is to pre-bias the spin such that the force preferentially "points towards the center" of the phase space, in a way that conserves the envelope of the state. This can be done with a pulse

$$U_r = e^{-i\sqrt{\pi}/2\hat{q}\hat{\sigma}_x} e^{i\epsilon\hat{p}\hat{\sigma}_y},$$

see figure 35 and exercises.

11.3.3 Quantum Error Correction

If you're experimentally inclined, you must be thinking that these encodings are completely ridiculous, even though they are quite elegant. We are talking about encoding information into squeezed states, which are typically used

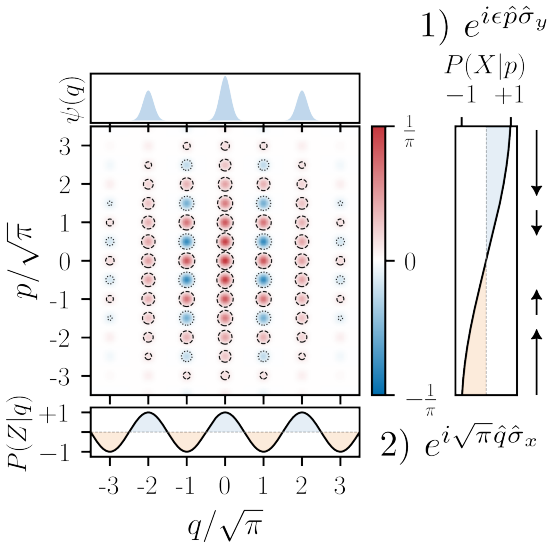

Figure 35: Biasing the qubit allows compensating for the envelope shift. For details see *Improved readout of qubit-coupled Gottesman–Kitaev–Preskill states*, Hastrup et al.

in metrology/sensing applications because they are hyper-sensitive to environmental fluctuations. While these concerns are valid, they turn out not to be quite true, and GKP state encodings perform very well at error correction, even at finite energy.

There are two main categories of quantum error correction protocols for GKP states. The first category employs an ancilla qubit (think a transmon dispersively coupled to a cavity, or an internal two-level system of an ion). This is also the only category that has been realized. The second category is based on homodyne detection techniques, which are typically found in optical systems. We will now discuss the first category.

Let's think a bit what it means to perform error correction in a GKP state. Our goal should be to sense that a displacement/phonon loss or gained happened, and then somehow correct for it. Let's try measuring a stabilizer using a state-dependent force and a finite-energy pulse of length ϵ_2 to see what happens.

$$U = e^{-i\sqrt{\pi}\hat{q}\hat{\sigma}_x} e^{i\epsilon_2\hat{p}\hat{\sigma}_y}.$$

If you recall the exercise sheet, we have after applying U and reading out the spin that (not accounting for Finite-energy)

$$\langle\hat{\sigma}_z\rangle = \langle\cos(2\sqrt{\pi}\hat{q})\rangle, \quad \langle\hat{\sigma}_y\rangle = \langle\sin(-2\sqrt{\pi}\hat{q})\rangle$$

This is interesting: reading out $\hat{\sigma}_z$ would tell us if we are in a GKP state or not. On the other hand knowing $\hat{\sigma}_y$ tells us if we are at the center of our Voronoi cell (i.e. if an error happened) or if we are at the edge of it. In this manner, the error information is mapped into the $\hat{\sigma}_y$ basis, see figure 36.

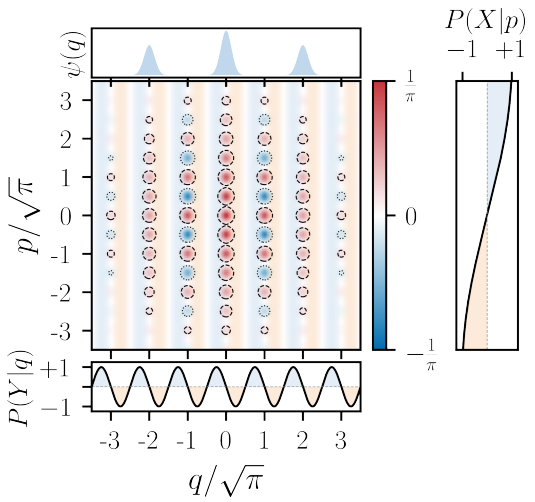

Figure 36: $P(X|p)$ is the expectation value of σ_x given a position p after the envelope compensation pulse. $P(Y|q)$ is the expectation value of σ_y after the stabilizer length pulse, which then turns the spin towards the nearest lattice point, such that the feedback pulse μ can correct for the error.

What remains is to perform feedback in order to correct for errors, and here once again we resort to a state-dependent force. Since we now mapped the error (displacement direction) information into the σ_y basis, we can use a state-dependent force pushing the state back to the center. This force has to readout σ_y and push along $\hat{q}$, i.e. it has the form $e^{i\mu\hat{p}\sigma_y}$. μ should be sufficiently small, and it turns out that the optimal parameters are $\epsilon_2 = \mu = \sqrt{2\pi}\Delta^2$.

Bringing all together, the protocol to correct for displacement errors along the q quadrature therefore is

$$U_q = e^{i\mu\hat{p}\sigma_y} e^{-i\sqrt{\pi}\hat{q}\hat{\sigma}_x} e^{i\epsilon_2\hat{p}\hat{\sigma}_y}.$$

A correction along p can be found by turning the phase space by 90°, such that

$$U_p = e^{-i\mu\hat{q}\sigma_y} e^{-i\sqrt{\pi}\hat{p}\hat{\sigma}_x} e^{-i\epsilon_2\hat{q}\hat{\sigma}_y}$$

Once this sequence (U_q or U_p) has been executed, the qubit needs to be reset. The reset provides the necessary removal (the error gets erased as the qubit gets reset). It can be understood analogously to sideband cooling, where now the subspace into which one cools is a two-dimensional subspace (the GKP qubit

subspace) rather than one-dimensional ($|n=0\rangle$). This leaves us with a final sequence of the form

$$U_q \rightarrow \text{ reset } \rightarrow U_p \rightarrow \text{ reset } \rightarrow U_q \rightarrow \text{ reset } \rightarrow ...$$

This error correction protocol is called the small-big-small protocol[13]. It brings a few subtleties that make it distinct from regular stabilizer codes, such as for example a surface code approach. One distinction is that it is a "trickle-down" method. That is that the length/weight of the error corrected is always the same, unlike in a stabilizer code that could for example distinguish a weight-1 and a weight-2 (1 vs 2 qubit) error.

To continue the parallel with the surface code, the analogon to the distance of the surface code is the energy of the codeword Δ. A higher energy allows a more accurate measurement of the errors. However unlike the case of the surface code, the GKP code does not admit a threshold: for any noise profile, there is always an optimal energy parameter. Below I give some numerics for a generic experiment, where a small-big-small protocol is ran at an arbitrary rate and the energy parameter scanned.

This phenomenon can be understood by looking again at the heating and loss channel:

$$\mathcal{E} = \left\{ \mathbb{1} - \frac{\bar{\kappa} dt}{2}(2\hat{a}^\dagger \hat{a} + 1), \sqrt{\bar{\kappa} dt}\hat{a}^\dagger, \sqrt{\bar{\kappa} dt}\hat{a} \right\}.$$

Since $\hat{a}\,|n\rangle = \sqrt{n}\,|n\rangle$, the larger the energy, the more likely it is that an error occurs given a certain error correction rate.

This has practical consequences: it means that even with a very good GKP state, there are no fault-tolerance/threshold guarantees. So to perform an arbitrary long calculation, one would arbitrarily good physical systems (unlike with codes that admit thresholds). This also means that one needs to concatenate the GKP code into a discrete-variable code, similarly to how cat codes can be concatenated into a repetition code. The line of research being pursued is to have very good GKP states, at the 10^{-9} error level, such that only very simple discrete outer codes are needed.

Experimentally, the small-big-small protocol has been used to perform beyond-break even error correction in a superconducting bosonic cavity mode encoding of qubits and qudits, and has been demonstrated in trapped ions on a single qubit as well as on a Bell state of two qubits[14].

11.3.4 Single-qubit Gates

Single-qubit gates are needed to perform useful computation, and two ingredients are needed: Clifford and non-Clifford gates. Clifford gates include X and Z

[13] See *Stabilization of Finite-Energy Gottesman-Kitaev-Preskill States*, Royer et al.
[14] see Sivak et al, Brock et al, de Neeve et al and Fontboté-Schmidt et al.

gates, while non-Clifford gates include can be realized by teleporting a magic (T) state into the code. While covering exact techniques for implmementing them is out of the scope of this lecture, I want to mention how one would implement them in a GKP state.

First, Clifford gates. It turns out that we already have implicitely done clifford gates in the small-big-small protocol! Let's consider again the stabilizer pulse. We can decompose it as

$$e^{-i\sqrt{\pi}\hat{q}\hat{\sigma}_x} = |+\rangle\langle+| \otimes e^{i\sqrt{\pi}\hat{q}} + |-\rangle\langle-| \otimes e^{-i\sqrt{\pi}\hat{q}} = |+\rangle\langle+| \otimes \hat{Z} + |-\rangle\langle-| \otimes \hat{Z}^\dagger$$

which using that $\hat{Z} = \hat{Z}^\dagger$ gives us exactly a single qubit gate on the GKP subspace

$$|+\rangle\langle+| \otimes \hat{Z} + |-\rangle\langle-| \otimes \hat{Z}^\dagger = \mathbb{1}_2 \otimes \hat{Z}.$$

This also means the small-big-small protocol has to run an even number of times to be a identity operator, otherwise it changes the Pauli frame. So using small-big-small we can do single-qubit gates, e.g. to do a Z gate we would do a protocol of the form:

$$U_q \rightarrow \text{ reset } \rightarrow U_q \rightarrow \text{ reset } \rightarrow U_p \rightarrow \text{ reset } \rightarrow U_q \rightarrow \text{ reset } \rightarrow ...$$

or written as the action of the Pauli operators

$$\hat{Z} \rightarrow \text{ reset } \rightarrow \hat{Z} \rightarrow \text{ reset } \rightarrow \hat{X} \rightarrow \text{ reset } \rightarrow \hat{Z} \rightarrow \text{ reset } \rightarrow \cdots -$$

Secondly, T states can be teleported into the code from an ancilla qubit, where they are more easy to prepare[15].

11.3.5 Two-qubit Gates

Finally, we want to connect these qubits with each other, and for that we require a two-qubit gate. How would a unitary that performs a two-qubit gate even look like? Let's construct a controlled-not as an example. The controlled not gate flips a target qubit's state ($\hat{X}_2$) if the control qubit is in a $\hat{Z}_1 = +1$ eigenstate.

A way to write this is via the unitary

$$CX = e^{i\hat{q}_1\hat{p}_2}.$$

Let's understand it better. If the control qubit (1) is in a 0 state, then we necessarily have $q_1 = 2n\sqrt{\pi}$ for a certain $n \in \mathbb{Z}$. One can view the gate as a displacement of the target qubit by the control qubit's position. If the target qubit is in $|0\rangle$, then the target qubit's $\hat{q}_2$ quadrature is displaced by $q_1 = 2n\sqrt{\pi}$ which is an identity on the codespace. If however the control qubit was in a 1 state, then we have that $q_1 = (2n+1)\sqrt{\pi}$ and the target's q_2 quadrature is displaced by an odd lattice spacing, which is exactly an $\hat{X}$ gate.

[15] see *Encoding a qubit in a trapped-ion mechanical oscillator* Flühmann et al,

This gate also has the effect of convoluting the states together (a similar effect happens from the control on the target qubit) such that the resulting finite-energy state has a broader envelope, see figure 37. This broadening can be corrected by the small-big-small protocol however, and reasonable gate fidelities can theoretically be achieved.

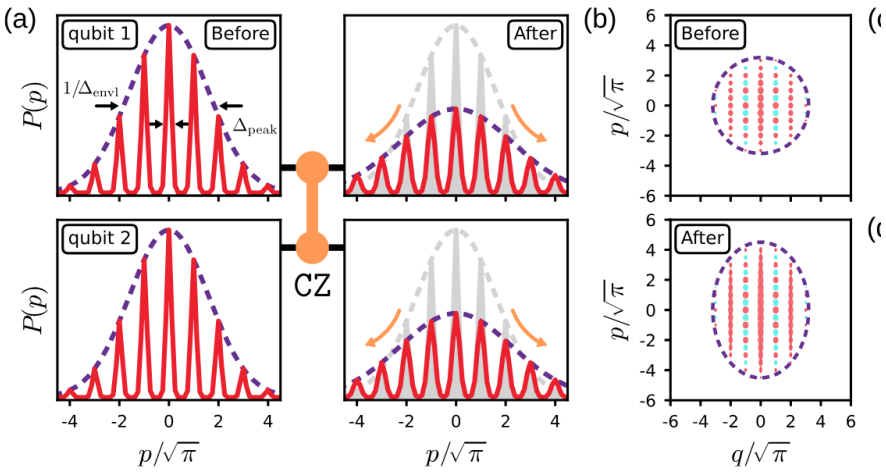

Figure 37: How a CZ gate broadens the quadrature. From *Two-qubit operations for finite-energy Gottesman-Kitaev-Preskill encodings*, Rojkov et. al

This type of CZ has not yet experimentally been achieved. What has been demonstrated however, is a type of CZ that uses an ancilla qubit as a mediator between the modes and an optimal control sequence to perform a CZ[16].

[16]see *Universal quantum gate set for Gottesman–Kitaev–Preskill logical qubits*, Matsos et al.